

ACOUSTIC IMAGING USING BISPECTRAL HOLOGRAPHY

A Thesis

Submitted In Partial Fulfilment of the Requirements

**for the Degree of
MASTER OF TECHNOLOGY**

By

B. R. K. REDDY

to the

DEPARTMENT OF ELECTRICAL ENGINEERING

INDIAN INSTITUTE OF TECHNOLOGY, KANPUR

AUGUST, 1980

ACOUSTIC IMAGING USING BISPECTRAL HOLOGRAPHY

A Thesis

Submitted In Partial Fulfilment of the Requirements

**for the Degree of
MASTER OF TECHNOLOGY**

By

B. R. K. REDDY

to the

DEPARTMENT OF ELECTRICAL ENGINEERING

INDIAN INSTITUTE OF TECHNOLOGY, KANPUR

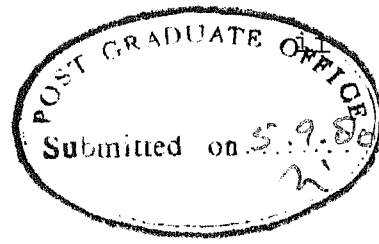
AUGUST, 1980

EE-1980-M-RED-A60

CENTRAL LIBRARY

Acc. No. A 66956

- 7 SEP 1981



CERTIFICATE

This is to certify that the thesis entitled,
'Acoustic Imaging using Bispectral Holography' is a
record of the work carried out under my supervision
and that it has not been submitted elsewhere for a
degree.

August 1980

S. K. Mullick
Dr. S.K. Mullick
Professor
Department of Electrical Engineering
Indian Institute of Technology
Kanpur

ACKNOWLEDGEMENT

I wish to express my profound gratitude to Dr. S.K. Mullick who introduced me to this field, and for his constant guidance and inspiration. I am greatly indebted to him for the invaluable encouragement and help given throughout my course of study. My association with him has been fruitful as well as memorable.

I would like to thank my friends Mr. R.V. Chalam and Mr. N. Gopinath, who helped me in the preparation of this report.

Thanks are due to Mr. K.N. Tewari for his neat and efficient typing of this thesis.

Kanpur

B.R.K. Reddy

August 1980.

CONTENTS

| | | Page | |
|------------|-----|---|----|
| CHAPTER | 1 | INTRODUCTION | 1 |
| CHAPTER | 2 | CONVENTIONAL HOLOGRAPHY | 15 |
| | 2.1 | Recording Process for Optical Signals | 15 |
| | 2.2 | Reconstruction Process for Optical Signals | 18 |
| | 2.3 | Recording of an Acoustical Hologram | 20 |
| | 2.4 | Liquid Surface Holography | 22 |
| | 2.5 | Recording of the Hologram Employing Digital Signal Processing Methods | 25 |
| CHAPTER | 3 | BISPECTRAL HOLOGRAPHY | 28 |
| | 3.1 | Theory of Bispectral Imaging | 29 |
| | 3.2 | The Computational Procedure Involved in Estimating the Bispectral Density | 37 |
| CHAPTER | 4 | COMPUTER SIMULATION OF THE IMAGING MODEL | 45 |
| | 4.1 | Image Reconstruction of a Point Source | 45 |
| | 4.2 | Image Reconstruction of Two Adjacent Point Sources | 52 |
| | 4.3 | Image Reconstruction of an 'Uniformly Illuminated Patch' | 52 |
| CHAPTER | 5 | CONCLUSIONS AND SUGGESTIONS | 57 |
| | 5.1 | Suggestions for Future Work | 58 |
| | a) | Channel Characterization | 58 |
| | b) | Communication through a Randomly Time Varying Media | 60 |
| REFERENCES | | | 61 |
| APPENDIX | | | 64 |

ABSTRACT

In this report our main concern is Image reconstruction of the object, emitting acoustic signals, using bispectral holography. Recording of the hologram using conventional techniques as well as using bispectral analysis is given. Conventional method is employed for image reconstruction from the recovered hologram signal. The bispectral holographic imaging technique has the potential the oretical advantages of ideal recovery in the presence of noise and distorting medium. Computer simulation of this processing strategy carried out in this work confirms this.

CHAPTER 1

INTRODUCTION

Holography is a technique, meant for the purpose of recording and displaying an image in its true three-dimensional format. It is a synthesis of two branches of optics, namely, interferometry used in recording the hologram, and diffraction used to display the image. This technique of photography has come to be known as holography after the word 'hologram' coined by Gabor to describe the interferogram that is used to record the wavefront to be reconstructed. The initiation for this synthesis came from engineers and physicists working in the area of communications. In communications the analogies to interference and diffraction are respectively modulation and demodulation. It is obvious from this analogy that the information stored in an interference pattern (modulation) can be retrieved as a result of diffraction of light by the recorded interference pattern (demodulation).

In the following section a simplified discussion of holography based on interference and diffraction is undertaken. At first, the interference phenomena is studied. As shown in Fig. 1.1, a plane monochromatic wave is split into two equal amplitude plane waves which then traverse separate paths until they are recombined. If the mirrors and beam splitters are perfect and if the optical path lengths are equal, the

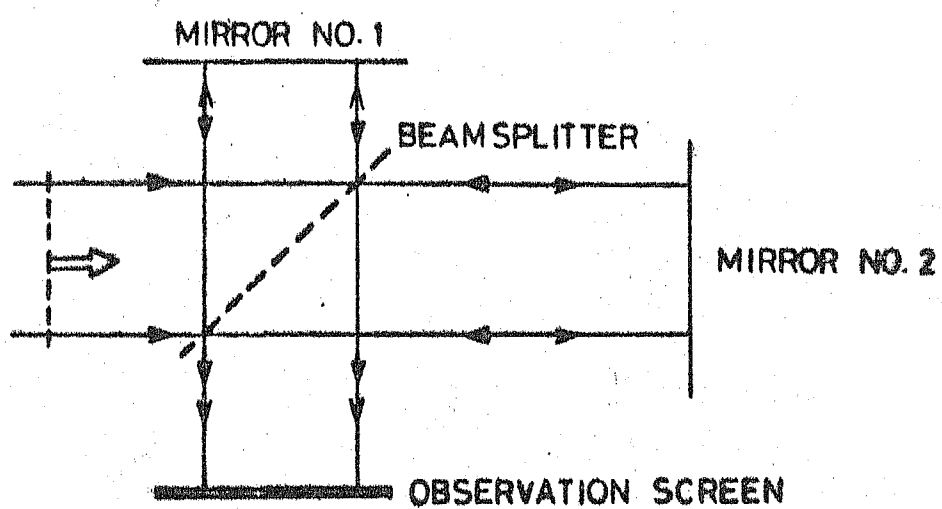


FIG. 1.1 MICHELSON INTERFEROMETER

output beam will be exactly like the input beam except for the loss in beam encountered at the beam splitter. A screen placed in the beam will therefore show uniform intensity.

If one of the mirrors is not quite parallel to the wavefront due to a misalignment, the reflected wave from it will combine with the other beam to form a linear system of fringes as shown in Fig. 1.2. Destructive interference occurs wherever the path length difference between the wavefronts is an odd multiple of half the wavelength.

If one of the mirrors is replaced with a concave parabolic reflector, the interference pattern we would expect to see is shown in Fig. 1.3. Note that this ring pattern shows decreasing spacing with increasing distance from the centre. This type of pattern is called Fresnel Zone pattern. If we impart a tilt to the spherical wave, we obtain a partial Fresnel Zone pattern as shown in Fig. 1.4.

When an aperture of some kind is interposed in a collimated beam of light, one might expect to see on the screen, a pattern of light sharply defined by the shadow of the aperture. Looking closely, however, the observer notes that some light exists in the shadow zone. The study of this phenomena is known as diffraction theory. The essence of the theory known as Huygens' principle is that each point on a wavefront can be considered as an elementary point radiating a spherical wavefront. When the elementary

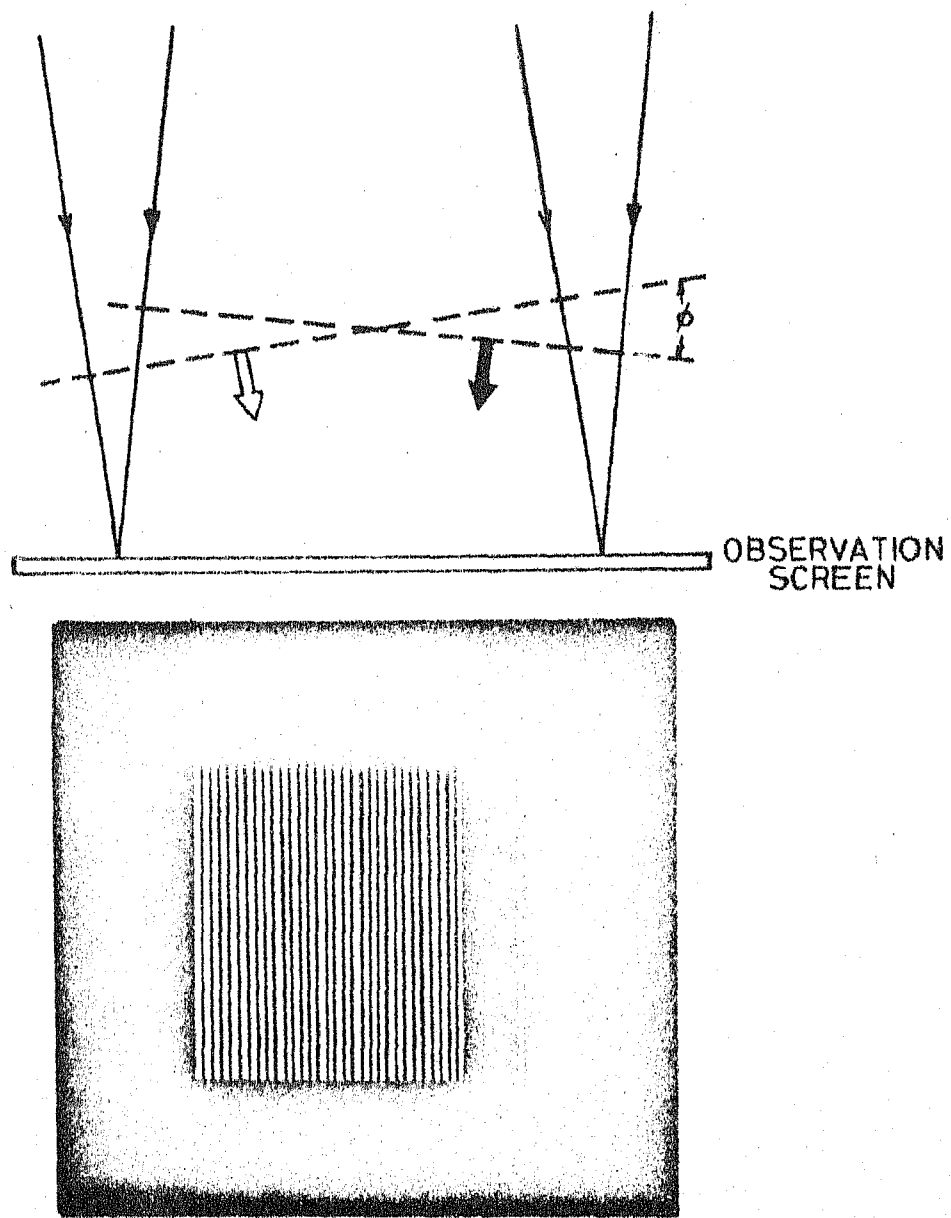


FIG.1.2 INTERFERENCE PATTERN OF TWO PLANE WAVES

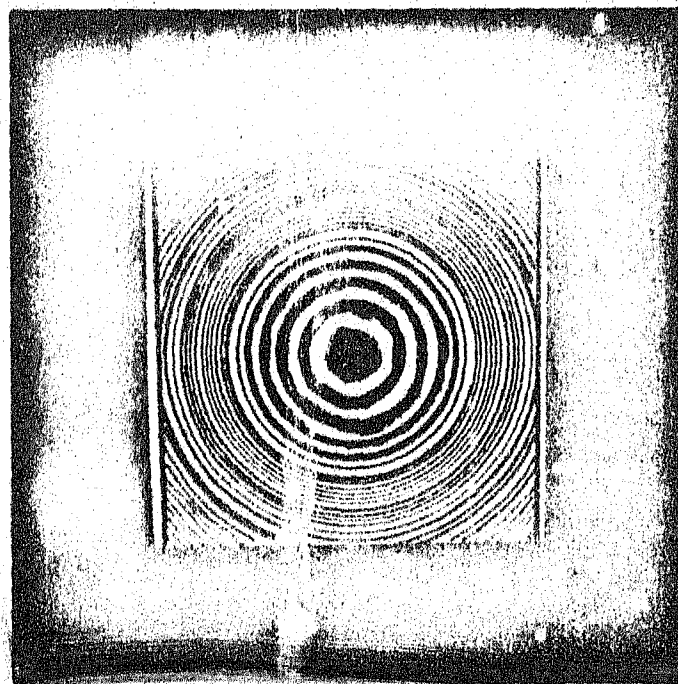
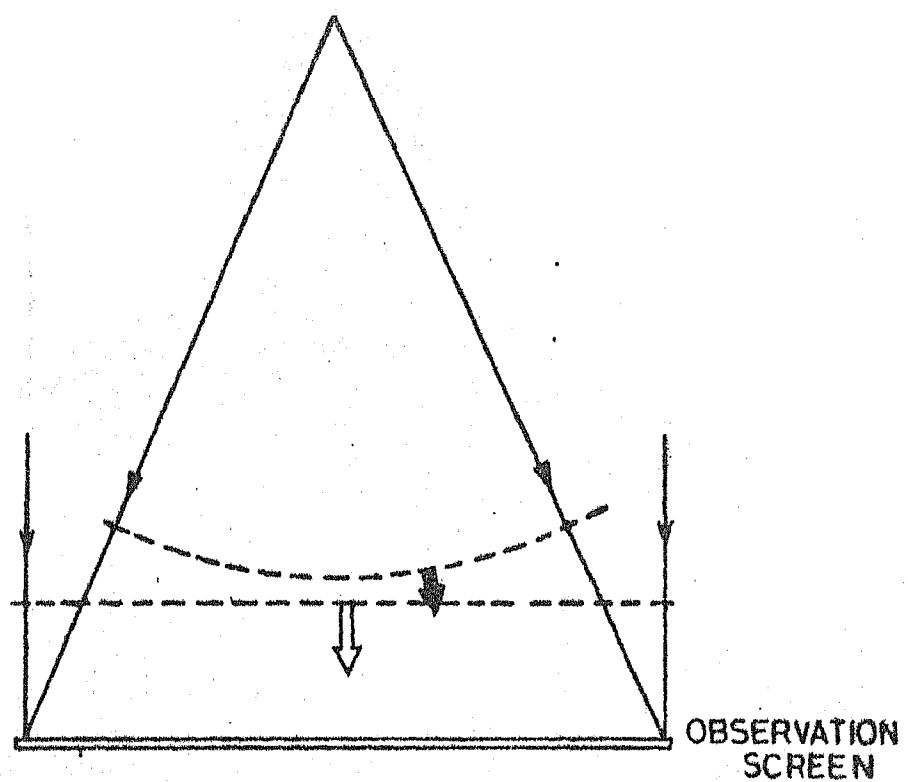


FIG.1.3 FRESNEL ZONE PATTERN

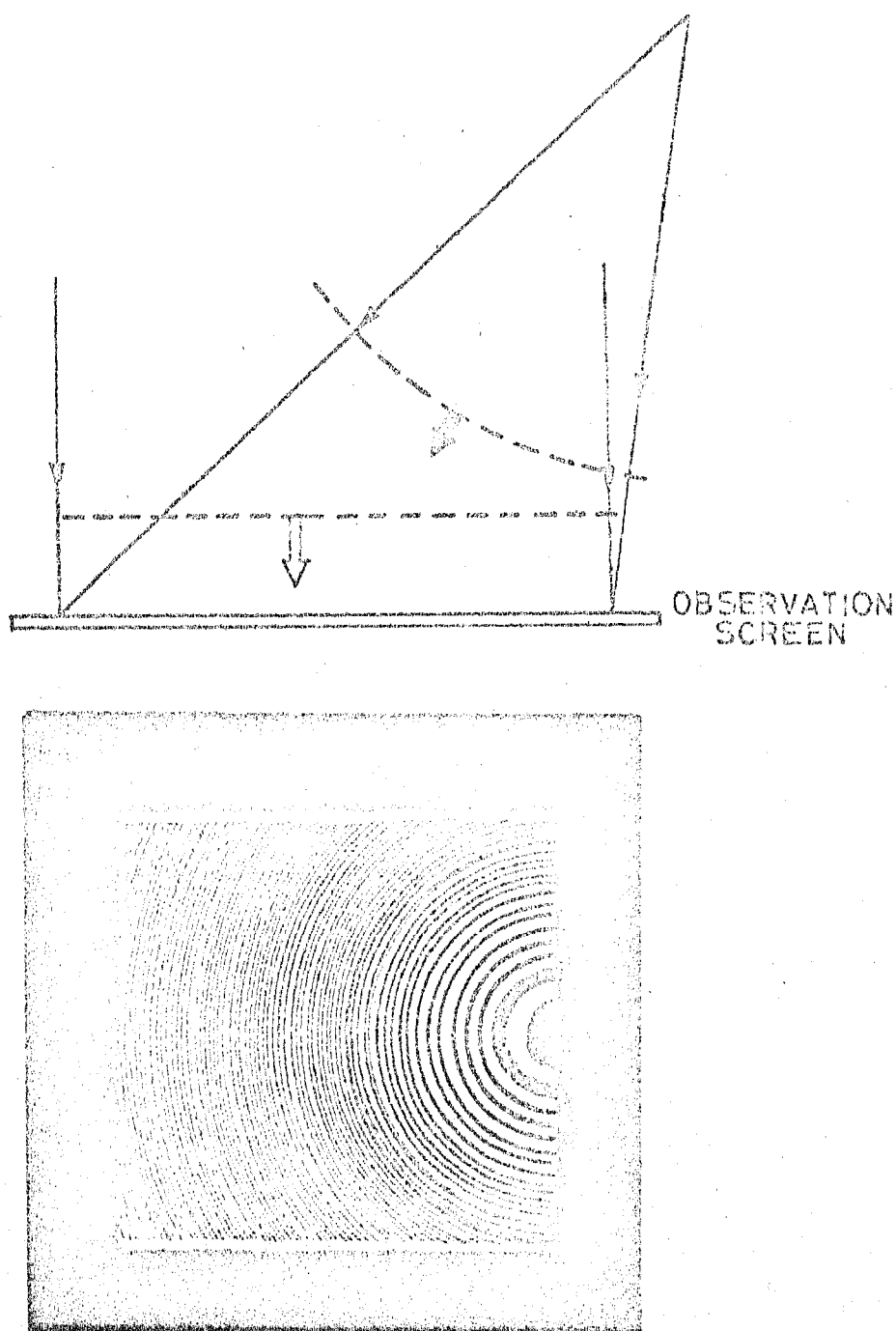


FIG.1.4 OFFSET FRESNEL ZONE PATTERN

wavelets are summoned in the prescribed manner the result is identical to the actual wavefront farther down stream. This principle is useful in analyzing the behaviour of the light in the presence of various types of apertures and obstructions.

A film containing the binary interference pattern generated in Fig. 1.2 is placed in the path of a collimated monochromatic light beam as shown in Fig. 1.5. In this figure we consider a single wavelet in the centre of each transparent space. Note that each circle represents an equiphasic surface advanced in phase by 2π from its neighbour to the left. The spatial separation of each surface from the next is one wavelength λ . We can draw a plane phase front tangent to the elementary wavelet phasefronts, three of which are shown in Fig. 1.5. For the binary pattern we can draw many more plane wavefronts at ever increasing angles. Comparing Fig. 1.5 with Fig. 1.2, we see that we have reconstructed the beams that made the interference pattern in the first place, with one exception; we have an extra beam at the conjugate angle.

The second example of the interference pattern was the Fresnel Zone pattern (Fig. 1.3). Fig. 1.6 shows what happens when this is illuminated. The Fresnel Zone pattern is, in effect, a locally linear grating, acting much the same way as our first example, except that the spacing varies as described previously. Hence the locally diffracted light changes in direction and the total effect provides a spherical

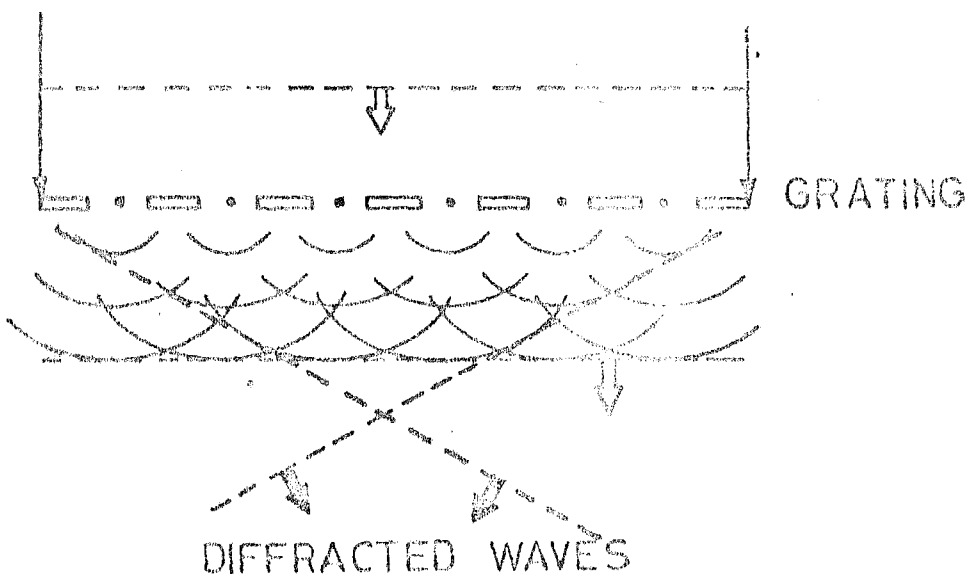


FIG.1.5 RECONSTRUCTION OF THE PLANE WAVES
THAT MADE THE INTERFERENCE PATTERN
IN FIG.1.2

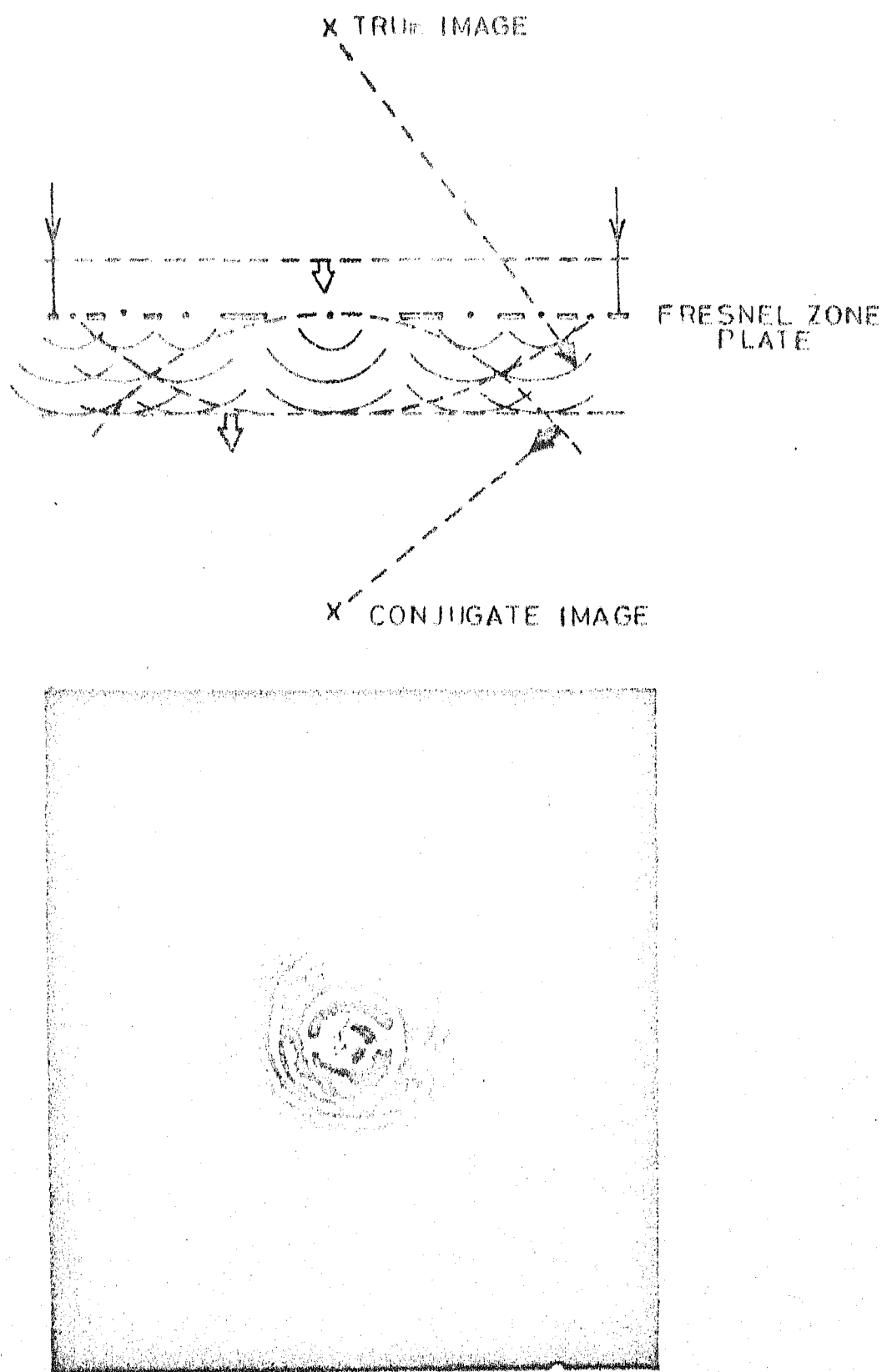


FIG.1.6 HUYGENS' RECONSTRUCTION OF THE FRESNEL ZONE PATTERN

wavefront, again duplicating the beams that caused the original interference pattern. Again we have an extra wave of opposite curvature.

The last example considered was that of an offset Fresnel Zone pattern (Fig. 1.4). For completeness we show in Fig. 1.7, the result of introducing this pattern in a beam of light, although one can anticipate the consequences.

The significance of the foregoing discussion is that interferometry has always had the capacity of recording a wavefront and later reconstructing it. These three examples chosen above clearly explain how holography works. The first example (Fig. 1.2) was intended to demonstrate both interference and diffraction. The second example (Fig. 1.3), a slightly more complicated situation, was chosen to show how Gabor Holography works and why it is not successful. Using the Gabor approach, one is reconstructing three beams of light, all occupying the same volume. That is, if one considers Fig. 1.6, one is forced to look at the plane wave and the converging extraneous wave both of which tend to mask the light from the desired wave, when looking for the replica of the spherical wave used in making the interferogram.

The third example, Fig. 1.4, shows how this difficulty is overcome by using an offset in the spherical beam. The same result can be produced by bringing the plane reference wave in at an angle, although in this case the interference

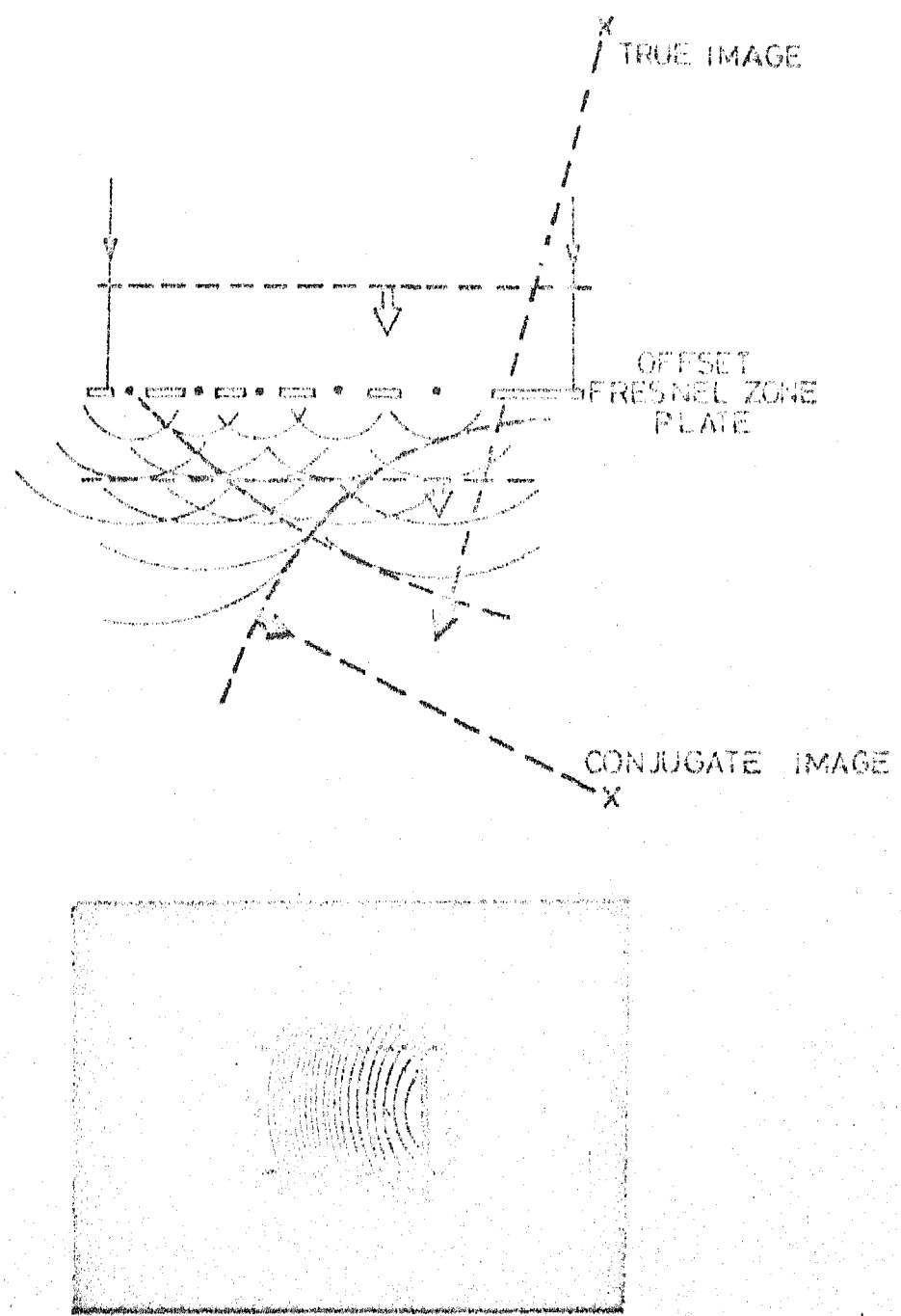


FIG.1.7 HUYGENS' RECONSTRUCTION OF THE OFFSET FRESNEL ZONE PATTERN

pattern is not a circular Fresnel pattern. In this case, all the three diffracted beams are separated in space, thus completely solving the problem of overlap.

To make these discussions conform to what one generally likes to think of as holography, one further step is required, namely, to record and display an image of a complicated object. This step only requires that we accept Huygens' principle which states that any arbitrary wavefront representing the light reflected from a complicated object can be considered to be the sum of a large number of point sources distributed over that wavefront. Since we have shown that we can image a single point or a spherical wave, it is reasonable to suppose that a distribution of points can also be imaged.

The foregoing theory depends upon the overriding principle; that is, that the two beams must be capable of interfering. This, in turn, requires a property of light, known as coherence. A wave is said to be perfectly coherent if its phase structure is fixed with respect to time. The degree of coherence of wave influences the recording of interference fringes and consequently the formation of hologram. In recording a wavefront, the sensitivity or time constant of the detector determines the integration time necessary for recording of interference fringes. If the relative phase of the wave changes during the recording time, the fringes move and quality of the recording is degraded. If the phase of the wavefront fluctuates randomly, the

recording of fringes is best described in terms of the mutual coherence function which is defined as the cross-correlation of the complex functions describing the wave at two points in space at different times under the assumption that waves are all polarized in the same sense and stationary in time. Lasers are commonly thought of as single frequency, highly coherent optical sources. However, they are often multiple frequency sources with relatively low coherence. By proper precautions and controls, a laser with a temporal and spatial coherence properties can be obtained. Sources for Microwave and acoustical wavelengths are normally coherent.

So far we have discussed optical holography but our main interest in this thesis is in some aspects of acoustical holography. First, we will see what are acoustic signals. The term 'Acoustic' applies to all mechanical vibrations and compressional and shear waves having any frequency. A very broad spectral range is encompassed within the field of acoustics. Any mechanical vibration with frequencies ranging from a lower limit of almost 0 Hz to an upper limit of 10^{12} Hz is within the realm of consideration.

Now we will relate the acoustical holography to optical holography. It should be noted that the interference and diffraction are phenomena common to all forms of energy whose propagation can be described in terms of a wave motion. All that is required is the ability to record an interference pattern in the particular type of radiation we happen to be

using and use this pattern to diffract light into a replica of the original wave. In this way it is possible to produce a visual image of an object irradiated with invisible energy.

Photographic film is insensitive to acoustic radiation. Point by point sampling method using one or more acoustical receivers and liquid surface holography are some of the methods developed for recording the acoustic hologram. The recording procedure of these methods is explained in detail in the second chapter.

Thus we have studied the recording of the hologram and reconstruction of the original wave (object wave) on a qualitative physical basis in this Chapter. Chapter 2 deals with the hologram recording and image reconstruction, in mathematical terms. The third chapter discusses the basic principle behind the bispectral passive imaging and the computational aspects involved in estimating the bispectral density. The fourth chapter presents the simulation work that has been done for the reconstruction of images of some idealized objects. The fifth and final chapter discusses the computational results and recommendations for future work. The computer programmes are listed in the Appendix.

CHAPTER 2

CONVENTIONAL HOLOGRAPHY

In Chapter 1, how a modified form of interferometry could be used to record a wavefront was discussed on a qualitative physical basis. This record, in turn could be used to reconstruct the wavefront by the process of diffraction. This method of photography has come to be known as holography after the word 'hologram' coined by Gabor to describe such an interferogram. In this chapter the process is described in mathematical terms.

2.1 Recording Process for Optical Signals

Consider two beams of radiation intersecting on a detecting plane as shown in Fig. 2.1. These two waves come from two transducers driven by the same oscillator. We can describe the optical field at a point (x, y) on the detecting surface due to beam 1 as

$$S_1(x, y) = a_1(x, y) \cos[\omega t + \varphi_1(x, y)] \quad (2.1)$$

and the field at (x, y) due to beam 2 as

$$S_2(x, y) = a_2(x, y) \cos[\omega t + \varphi_2(x, y)] \quad (2.2)$$

where $a(x, y)$ is the amplitude of the wave and $\varphi(x, y)$ is the phase of the wave. The total amplitude at (x, y) is the sum of these two individual beams. The result is

$$\begin{aligned} S(x, y) &= S_1(x, y) + S_2(x, y) \\ &= a_1(x, y) \cos[\omega t + \varphi_1(x, y)] + a_2(x, y) \cos[\omega t + \varphi_2(x, y)] \end{aligned} \quad (2.3)$$

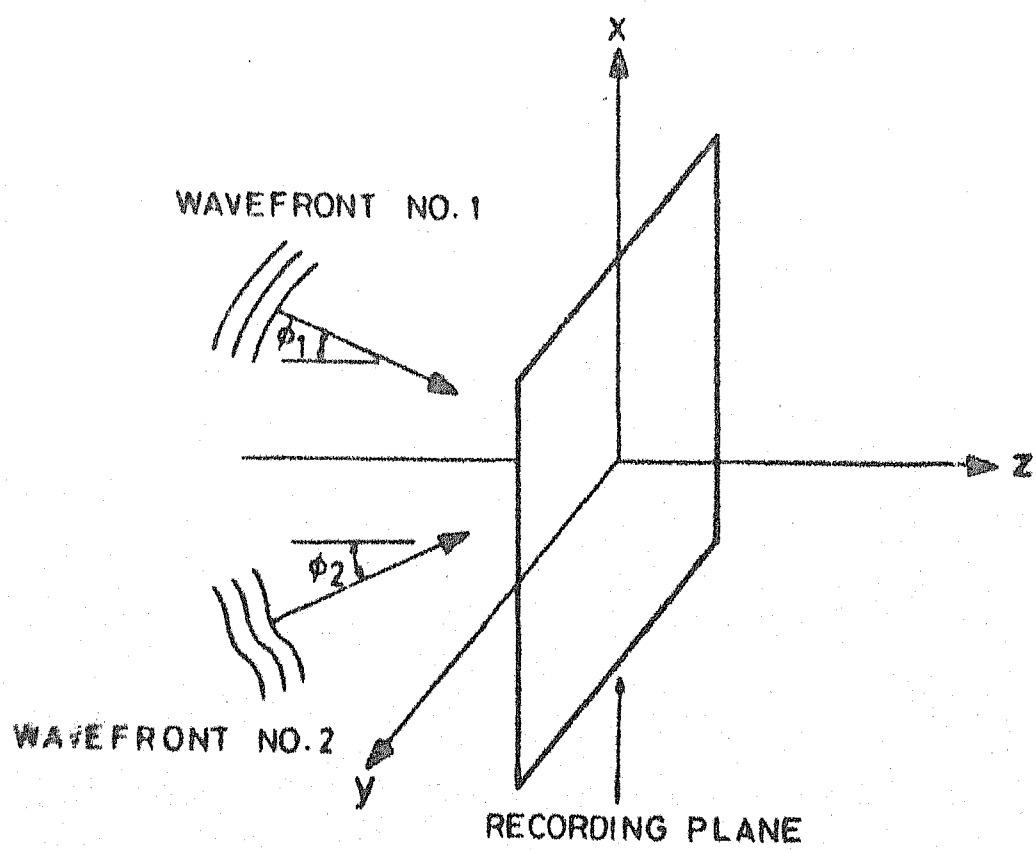


FIG. 2.1 FORMATION OF THE HOLOGRAM

Since no detector exists which can detect the oscillations at optical frequencies, the best that can be done is to measure the intensity. The signal that is actually recorded is therefore some function of intensity, which can be written

$$I(x, y) = \langle [S(x, y)]^2 \rangle_t \quad (2.4)$$

where $\langle \dots \rangle_t$ denotes a time average over many cycles of radiation.

Substituting eq.(2.3) into eq.(2.4) yields

$$I(x, y) = S_1^2 + S_2^2 + (S_1 S_2)_+ + (S_1 S_2)_-$$

where

$$\begin{aligned} S_1^2 &= \frac{1}{2} a_1^2(x, y) \langle [1 + \cos 2(\omega t + \varphi_1(x, y))] \rangle_t \\ S_2^2 &= \frac{1}{2} a_2^2(x, y) \langle [1 + \cos 2(\omega t + \varphi_2(x, y))] \rangle_t \\ (S_1 S_2)_+ &= \frac{1}{2} a_1(x, y) a_2(x, y) \langle \cos(2\omega t + \varphi_1(x, y) \\ &\quad + \varphi_2(x, y)) \rangle_t \\ (S_1 S_2)_- &= \frac{1}{2} a_1(x, y) a_2(x, y) \langle \cos(\varphi_1(x, y) - \varphi_2(x, y)) \rangle_t \end{aligned} \quad (2.5)$$

This equation clearly shows why the temporal frequency term is so easily dropped. An oscillating function such as $\cos(\omega t)$ averages to zero, if many cycles are considered. Hence, eq.(2.5) reduces to

$$I(x, y) = \frac{1}{2} \{ [a_1^2(x, y) + a_2^2(x, y) + a_1(x, y) a_2(x, y) \cos(\varphi_1(x, y) \\ - \varphi_2(x, y))] \} \quad (2.6)$$

Note that we have succeeded in preserving phase information even though the recording was done on a phase insensitive medium. This, of course, is the secret of holography.

2.2 Reconstruction Process for Optical Signals

In Chapter 1, it is noted that the wavefront stored on the interferogram could be reconstructed by the process of diffraction of a plane wave. This plane wave can be expressed as

$$S_3(x, y) = a_3(x, y) \cos(\omega t + \varphi_3(x, y)) \quad (2.7)$$

Suppose we have exposed a photographic plate to the intensity shown in eq.(2.6). After development it possesses a transmittance proportional to the intensity. Then the wave S_3 after passing through the plate is modified by it as

$$\begin{aligned} KI(x, y) S_3(x, y) = & \frac{K}{2} [a_1^2(x, y) + a_2^2(x, y)] a_3(x, y) \cos[\omega t + \varphi_3(x, y)] \\ & + \frac{K}{4} a_1(x, y) a_2(x, y) \{ \cos[\omega t + \varphi_1(x, y) - \varphi_2(x, y) \\ & + \varphi_3(x, y)] + \cos[\omega t - \varphi_1(x, y) + \varphi_2(x, y) + \varphi_3(x, y)] \} \end{aligned} \quad (2.8)$$

where K is a constant.

If we consider the terms one at a time we note that the first term represents the reconstruction wave modified in amplitude. The second term assuming that S_3 is a replica of S_2 , becomes

$$\frac{K}{4} a_2^2(x, y) a_1(x, y) \cos[\omega t + \varphi_1(x, y)]$$

which we recognise as the original wave, S_1 , modified in amplitude. If S_2 happens to be a plane wave, a_2 is a constant and a perfect reconstruction is obtained. With the same reconstruction wave the third term of eq.(2.8) becomes

$$\frac{K}{4} a_2^2(x, y) a_1(x, y) \cos[\omega t - \varphi_1(x, y) + 2\varphi_2(x, y)]$$

This is the extraneous term we referred to earlier. There are several more options available. For example, we could let S_3 be a replica of S_2 with opposite curvature; that is

$$S_3(x, y) = a_2(x, y) \cos[\omega t - \varphi_2(x, y)]$$

Then the second and third terms of eq.(2.8) become

$$\frac{K}{4} a_2^2(x, y) a_1(x, y) \cos[\omega t + \varphi_1(x, y) - 2\varphi_2(x, y)]$$

and

$$\frac{K}{4} a_2^2(x, y) a_1(x, y) \cos[\omega t - \varphi_1(x, y)]$$

Here we see that the last term becomes a reconstruction of S_1 with opposite curvature and the second term is the extraneous image. Another possible form of S_3 is S_1 , giving reconstructed terms.

$$\frac{K}{4} a_1^2(x, y) a_2(x, y) \cos[\omega t + 2\varphi_1(x, y) - \varphi_2(x, y)]$$

and

$$\frac{K}{4} a_1^2(x, y) a_2(x, y) \cos[\omega t + \varphi_2(x, y)]$$

Thus we have reconstructed S_2 and demonstrated the complete ambivalence of the interferometer. While recording the waveform of one arm we have also recorded the other. Hence either one may be reconstructed by diffracting the other beam through the interferogram. Additionally by using the conjugate of the one of the interfering beams as the diffracting beam we can reconstruct the conjugate of the other.

2.3 Recording of an Acoustic Hologram

In case of acoustic signals, because of their long wavelength, measuring the phase is not a difficult problem. Detectors capable of measuring the amplitude of oscillations of the acoustic signals are readily available. The system used, for recording the hologram is shown in Fig. 2.2. Here the received signal (scanned signal) is multiplied by the oscillator signal (reference signal) and sent through a low pass filter to yield the desired hologram signal. The mathematical procedure is as follows:

$$S_1(x, y) = a_1(x, y) \cos[\omega t + \varphi_1(x, y)] \quad (2.9)$$

After multiplication by $a_2 \cos(\omega t + \varphi_2)$, this becomes

$$S'(x, y) = \frac{a_2 a_1(x, y)}{2} \left\{ \cos[2\omega t + \varphi_1(x, y) + \varphi_2] + \cos[\varphi_1(x, y) - \varphi_2] \right\} \quad (2.10)$$

After low pass filtering, we are left with

$$S''(x, y) = \frac{a_2 a_1(x, y)}{2} \cos[\varphi_1(x, y) - \varphi_2] \quad (2.11)$$

Comparing eqs. (2.9) and (2.11) we see that we have succeeded in obtaining the same information without the attendant extraneous terms a_1^2 and a_2^2 .

The signal $S''(x, y)$ may be stored on a magnetic tape. The only way to get the full amount of information from this data is to reconstruct the wavefront. To do this, the data must be recorded in the form of a hologram. The basic method is to intensity modulate a light source with the stored signal.

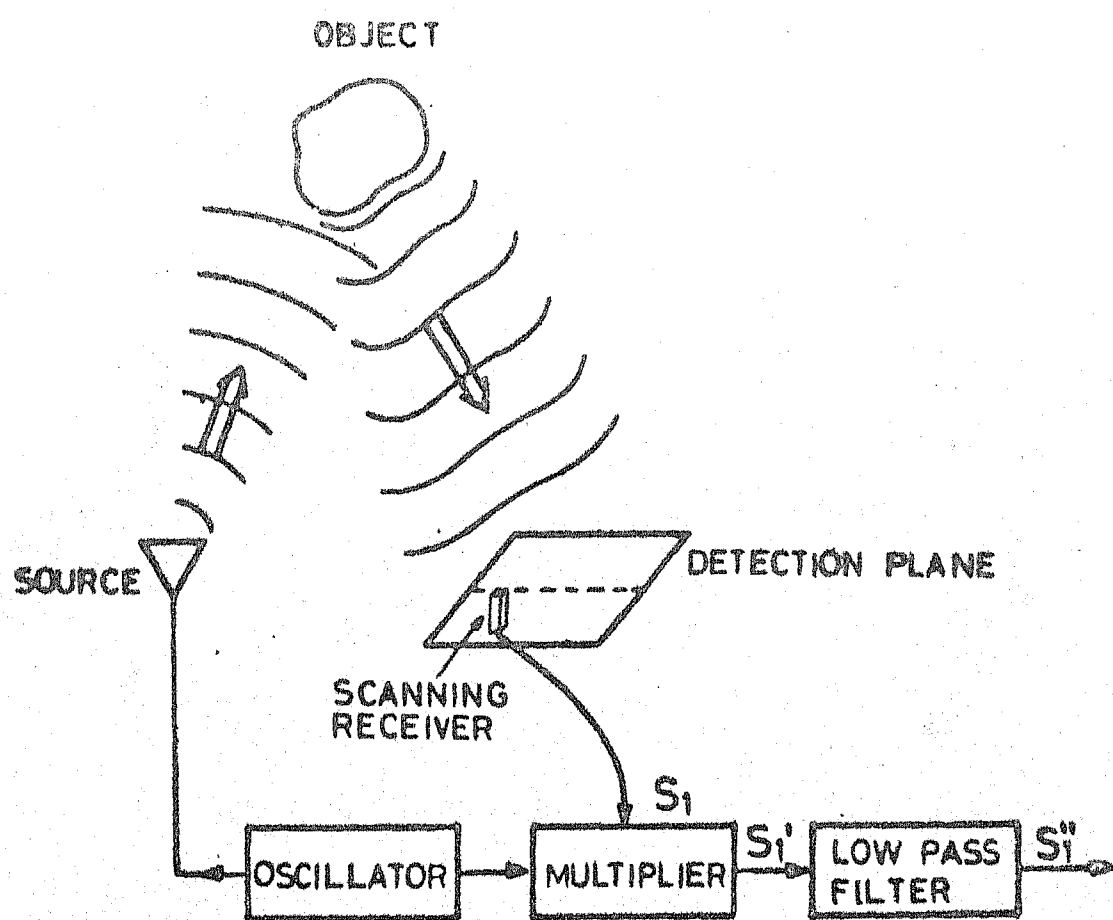


FIG. 2.2 AN ARRANGEMENT USED FOR RECORDING THE ACOUSTICAL HOLOGRAM

on magnetic tape about some average intensity, move it in position and velocity in proportion to that of the detector and record the light on a light-sensitive medium that is shaped proportionately to the surface over which the receiver was scanned.

In practice only planar surfaces have been used, but scan lines in the surfaces have been straight lines or circles. The most common light sources have been an incandescent bulb focussed to a very small point, and the face of a cathode ray tube with a moving intensity modulated spot. The first method requires a mechanical scanning system whereas the second one requires an electronic scanning system. Each method requires a camera to photograph the moving light source. Reconstruction process is same as the one explained for optical signals.

2.4 'Liquid surface holography'

'Liquid surface holography' is another means of recording the interference pattern. The system used for imaging is shown in Fig. 2.3. It includes an object beam transducer that insonifies the object uniformly. The object scatters, diffracts, absorbs energy, and modifies the phase distribution in the wave-front. A pair of acoustic lenses are used to image the sound distribution of the object into the plane of the hologram. The geometry of the wavefront of the reference beam should be simple so that the wavefront can be easily simulated in a beam of light. This means that the wavefront should be either plane or spherical. The object beam and the reference beam should be essentially coherent. The rapid response of the liquid surface

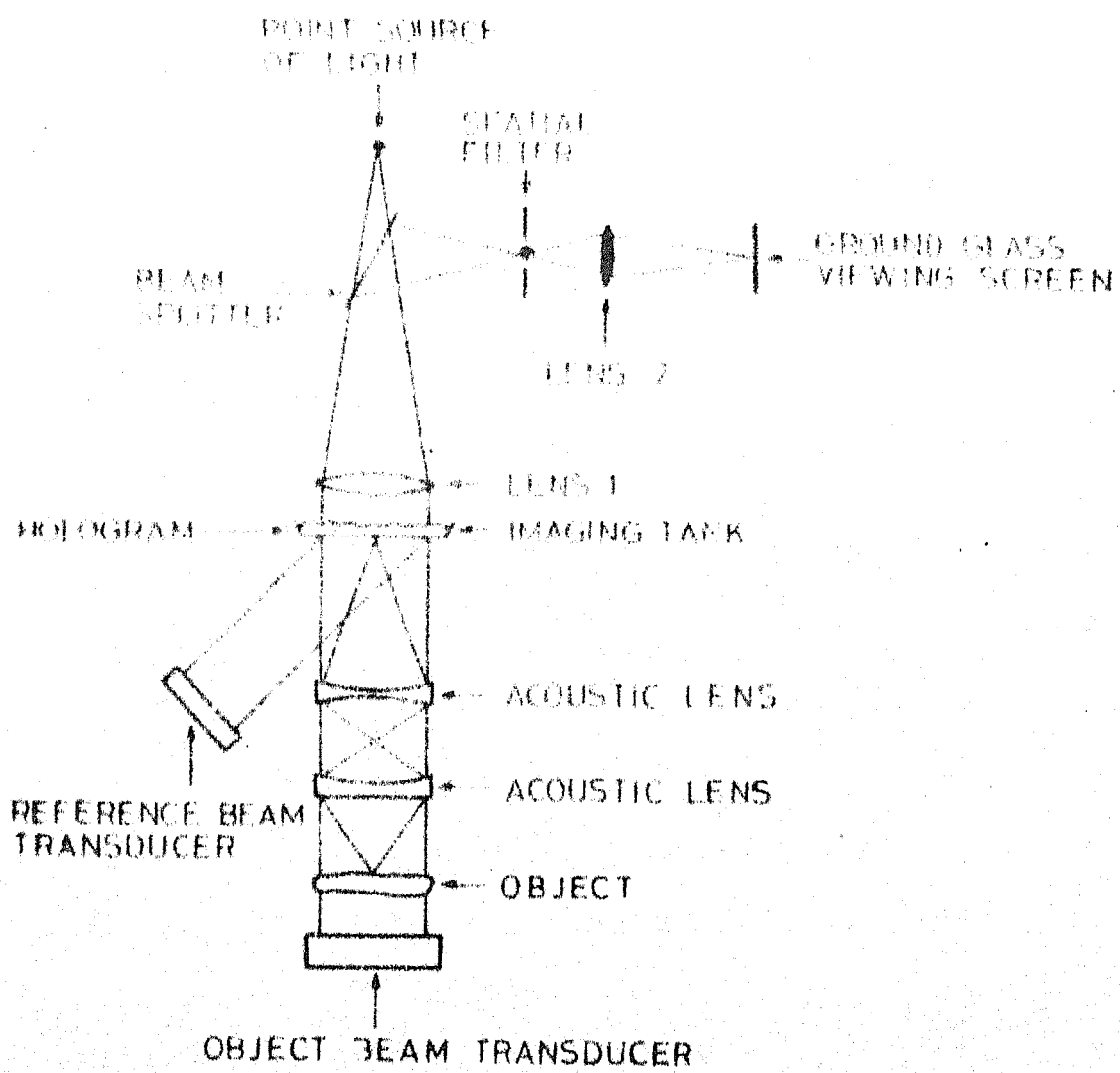


FIG. 2.3 AN ARRANGEMENT FOR IMAGING ULTRA SOUND BY USE OF LIQUID SURFACE ACOUSTICAL HOLOGRAPHY

permits a few percent difference in frequency between the object and the reference beams. The sound field of the object beam mixes with the sound field of the reference beam transducer to form an interference pattern at liquid-air interface in the imaging tank. The interference pattern is imprinted in the liquid surface as variations in elevation.

An imaging tank is used to isolate the hologram from liquid surface disturbances in the main (object) tank. Use of a imaging tank also allows the use of different liquids for hologram formation and for object immersion. Thus, liquids can be chosen which are optimum for each of these purposes.

The hologram surface imposes phase variations in the reflected beam of light which cause diffraction of the light. First order diffracted light is passed at the spatial filter which blocks all other light reflected from the hologram surface.

Lens 1 is used to image the point source of light at the plane of the spatial filter after reflection from hologram surface. Lens 2 images the hologram surface on the ground glass viewing screen. Since the hologram is a focussed image type, the ground glass screen displays the desired image of the object. Although the hologram modifies only the phase of the light, there is amplitude imaging because the amount of light diffracted into the first order varies as the amplitude of the interference pattern on the liquid surface, which in turn, varies as the amplitude of the wave in the object beam.

2.5 Recording of the Hologram Employing Digital Signal Processing Methods

An alternative solution for the reconstruction of the wavefront of the object wave is using digital signal processing methods. Here, we use two receivers; one is fixed and the other scans over a hologram plane.

The signal detected by the scanning receiver can be expressed as

$$s_1(t, x, y) = A(x, y) \cos[\omega t + \varphi_1(x, y)] + n_1(t)$$

where (x, y) is a point on the hologram plane and $n_1(t)$ is the additive Gaussian noise. $A(x, y)$ and $\varphi(x, y)$ are amplitude and phase distributions of the scanned signal.

The signal detected by the fixed receiver

$$s_2(t) = \text{reference signal} = B \cos(\omega t + \varphi_2) + n_2(t)$$

where $n_2(t)$ is additive Gaussian noise. Both $n_1(t)$ and $n_2(t)$ are assumed to be independent of the received signals, but not so in between them.

The cross-power spectral density between the object and reference waves is computed at all the scanned points on the hologram plane and is given by the following expression:

$$C_{s_1 s_2}(\omega, x, y) = A(x, y) B \cos(\varphi_1(x, y) - \varphi_2) + C_{n_1 n_2}(\omega)$$

where $C_{n_1 n_2}$ is cross-power spectral density between the noises $n_1(t)$ and $n_2(t)$.

It is clear from the above expression that the cross-power spectral density $C_{s_1 s_2}$ contains the amplitude and phase

information of the object wave. Hence the cross-power spectral density computed at each point on the hologram plane forms the hologram signal in the Fourier domain. The image is retrieved as a computer print-out, simply by performing an inverse Fourier transform on the hologram signal.

The signal processing carried out in the computer is shown in Fig. 2.4.

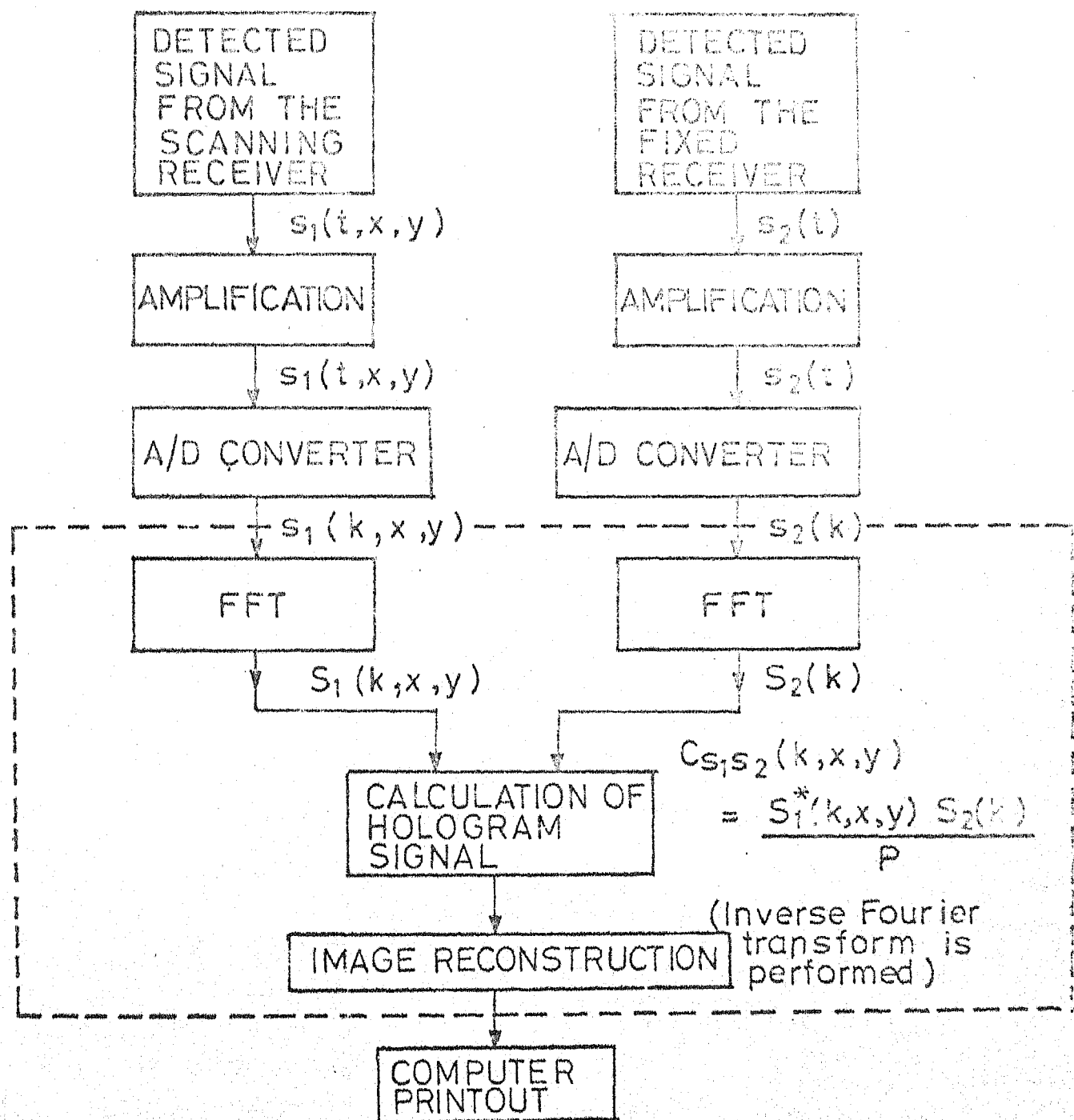


FIG.2.4 SIGNAL PROCESSING STEPS IN CONVENTIONAL DIGITAL HOLOGRAPHY

CHAPTER 3

BISPECTRAL HOLOGRAPHY

The amplitude and phase of the object wave can be obtained by cross correlating the object wave and reference wave on the hologram plane. This is the conventional way of recording the hologram, which was discussed in the last chapter. If the signals illuminating the object or object emitted signals are non-Gaussian the phase of the signals can be derived from bispectra or higher order spectral analysis. The condition that signal should be non-Gaussian is satisfied in many practical applications, since any periodic signal can be regarded as a non-Gaussian signal and self-emitting signals from objects such as complicated mechanical systems can also be considered as non-Gaussian signals.

Two receivers one fixed and the other scanning over the hologram plane are used to obtain the holographic information. Auto-bispectral and cross-bispectral analysis are carried out on the detected signals. By taking their ratio the required information is obtained. This is explained in the later parts of this chapter. Image reconstruction is performed by using conventional holographic methods.

Bispectral analysis provides a means of obtaining holograms free from additive Gaussian noises in the amplitude and shape of the power spectra.

The application of bispectral analysis is equivalent to the utilization of mutual relations among three frequency components, that satisfy $f_1 + f_2 + f_3 = 0$. In the case of a Gaussian signal each frequency component is independent. These facts produce very effective and special features when this method is applied to holographic imaging systems.

The principle of bispectral analysis for getting the hologram signal is dealt with in the following sequence. First the description of the data acquisition system and assumptions postulated for generalized object illuminating signals and additive noise are given. Secondly by discussing the properties of the bispectra of the signals detected at the hologram plane, the procedure required to obtain the hologram signal is derived. Finally the image reconstruction process is discussed briefly.

3.1 Theory of Bispectral Imaging[2]

Consider the system shown in Fig.3.1, where non-Gaussian random signals $S_i(p, t)$ ($i = 1, \dots, M$) are assumed to be emitted from the object plane π_1 . $n(t)$ is the noise added in the channel. These signals are received at the hologram plane π_2 by two receivers. One is a fixed receiver R_1 , which is assumed to be located at the origin and the other one is scanning receiver R_2 , located at r_2 on the same plane. $n_1(t)$ and $n_2(t)$ are the noises added to the detected signals at receivers R_1 and R_2 respectively. The signals on the

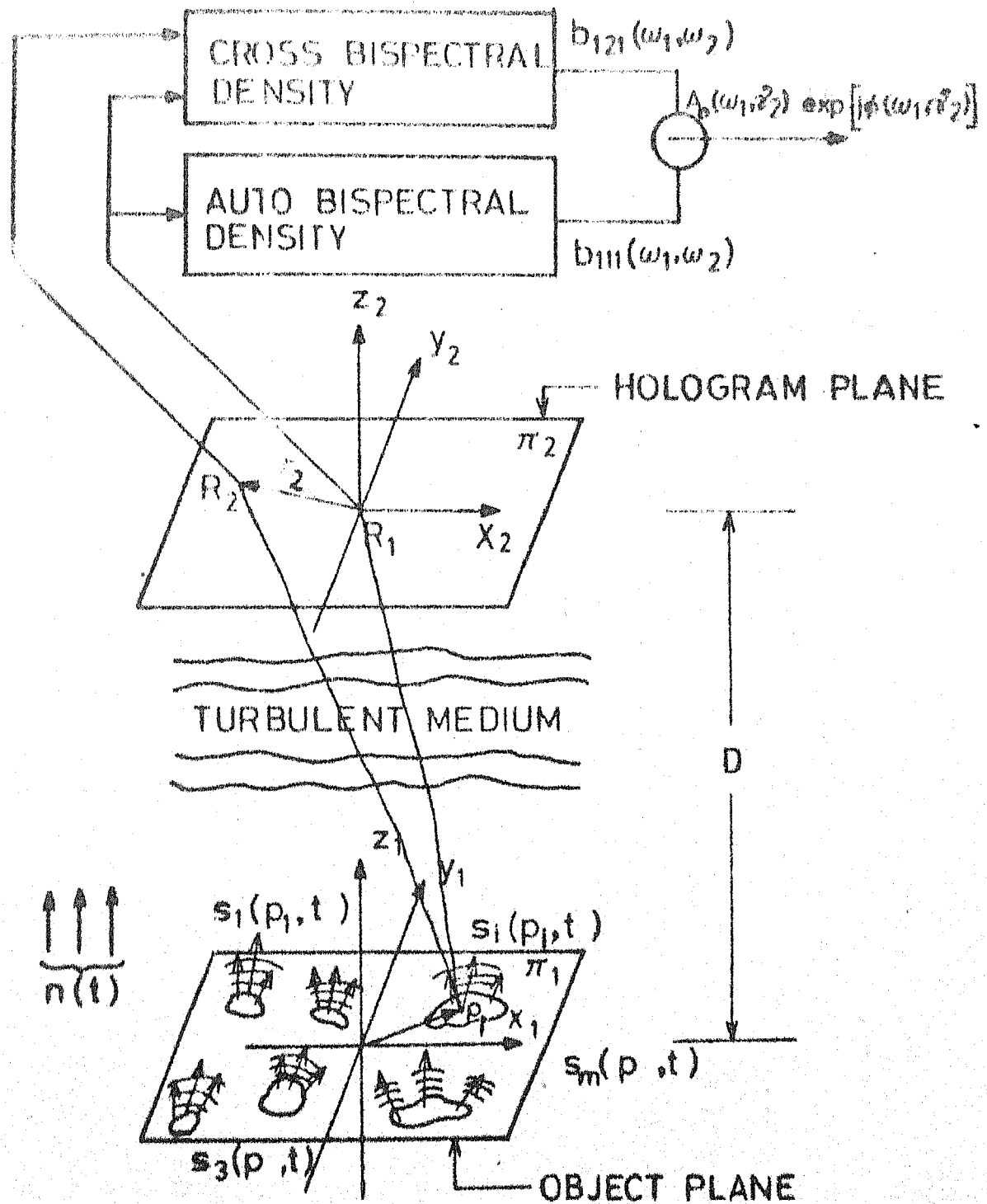


FIG. 3.1 SCHEMATIC CONSTRUCTION AND SIGNAL PROCESSING OF BISPECTRAL HOLOGRAPHY

plane π_2 may be considered as sum of the following three components.

- a) Signals from the object plane.
- b) Surrounding noises $n_s(t)$, $n(t)$.
- c) The additive noises $n_1(t)$, $n_2(t)$ which are added at the corresponding receivers.

Information about the amplitude and phase of the wavefront of a given frequency at each point on the hologram plane is required to construct the hologram.

Assumptions: The assumptions postulated for the object illuminating signals and the transmission medium are given below:

i) The object illuminating signals $s_i(p,t)$ ($i=1, \dots, M$) are harmonizable (this means that $s_i(p,t)$ can be expressed as the first expression of Eq.(3.1)) and third order weakly stationary non-Gaussian signals and without loss of generality they are assumed to have zero mean.

$$s_i(p,t) = \int_{-\infty}^{\infty} \exp(j\omega t) dZ_i(\omega)$$

$$\langle dZ_i(\omega) \rangle = 0 \quad (3.1)$$

$$b_i(\omega_1, \omega_2) d^2\omega = \langle dZ_i(\omega_1) dZ_i(\omega_2) dZ_i(\omega_3) \rangle_{\omega_1 + \omega_2 + \omega_3 = 0}$$

where $\langle \cdot \rangle$ denotes an ensemble averaging operation and

$b_i(\omega_1, \omega_2)$ represents the bispectral density of $s_i(p,t)$.

LIBRARY
Acc. No. A 66956

ii) Noises are assumed to be Gaussian. No restriction is made about their power spectra. It is also assumed that they are statistically independent of the object illuminating signals $S_i(t)$ ($i = 1, \dots, M$). No assumption is made about the independence among these noises.

The received signals $u_q(r_q, t)$ ($q = 1, 2$) at the two receivers can be expressed as follows:

$$u_q(r_q, t) = \int_{\pi_1}^{\infty} \int_{-\infty}^{\infty} \sum_{i=1}^M A_i(p) Z_i(\omega; p, r_q) e^{j\omega t} d\omega dp + n(t) + n_q(r_q, t), \quad q=1, 2 \quad (3.2)$$

where $A(p)$ is the amplitude of the object wave at a point p on the object plane and $H(\omega; p, r)$ is given by

$$\int_{-\infty}^{\infty} h(\tau, p, r) e^{-j\omega\tau} d\tau$$

where τ is the time instant at which you apply the input and r is an observation point on the hologram plane.

Under the assumption that turbulences of the medium affect only as random phase shifters on propagating waves and their variation in time are so slow that they can be regarded as fixed values while bispectral analysis for each data is carried out, the transfer function $H(\omega; p, r)$ is expressed as follows:

$$H(\omega; p, r) = \frac{G(\omega)}{j \lambda d(p, r)} \exp[-jkd(p, r)] \exp[ja(\omega; p, r)] \quad (3.3)$$

where λ , k denote respectively, the wavelength and wave-number of a wave with angular frequency ω ; $a(\omega; p, r)$ is the accumulated phase shift due to random medium between p and r ; $G(\omega)$ is the amplitude transmitting factor.

Another assumption made on channel is the accumulated phase shifts caused by random medium are subjected to the same probability distribution for any p and r , so that they are expressed as a random variable with index ω as $b(\omega)$.

The transfer function of the medium described above does not take the multipath effect into consideration. The reason for this is that the size of the random scatterers is much greater than a wavelength. Because of that the wave scattered by the particle is largely confined to a small angle in the forward direction.

Substituting $H(\omega; p, r)$ in Eq.(3.2), we get

$$u_q(r_q, t) = \sum_{i=1}^M \int_{-\infty}^{\infty} \left[\int_{\pi_1}^{\infty} \frac{G(\omega)}{j\lambda d(p, r_q)} A_i(p) \exp[-jkd(p, r_q)] \right. \\ \left. \exp[ja(\omega; p, r_q)] dp \right] \exp(j\omega t) dZ_i(\omega) + N_q(r_q, t) \\ q = 1, 2 \quad (3.3)$$

where $N_q(r_q, t)$ ($q = 1, 2$) are the overall corrupting noises at the receivers and they are independent of $s_i(p, t)$ ($i = 1, \dots, M$) from the assumption (ii). $A(p)$ is the amplitude of the emitting signal at a point p on the object plane.

Consider the signals $x_i(t) = X(t) + Y_i(t)$ ($i = 1, 2$) where $Y_i(t)$ ($i = 1, 2$) are weakly-stationary Gaussian signals

and $X(t)$ is a third order stationary non-Gaussian signal and independent of $Y_i(t)$ ($i = 1, 2$). Then the third order cross-correlation function $R_{X_1 X_2 X_1}(\tau_1, \tau_2)$ between $X_1(t)$ and $X_2(t)$ is given as follows:

$$\begin{aligned}
 R_{X_1 X_2 X_1}(\tau_1, \tau_2) &= \langle [X_1(t) - \langle X_1(t) \rangle] [X_2(t+\tau_1) - \langle X_2(t+\tau_1) \rangle] \\
 &\quad [X_1(t+\tau_2) - \langle X_1(t+\tau_2) \rangle] \rangle \\
 &= R_{XXX}(\tau_1, \tau_2) + R_{Y_1 Y_2 Y_1}(\tau_1, \tau_2) \\
 &= R_{XXX}(\tau_1, \tau_2)
 \end{aligned}$$

where the fact that the third order correlation function of any Gaussian signal is identically zero is used.

By applying this relation to $u_q(r_q, t)$ ($q = 1, 2$) in Eq.(3.3), the third order cross-correlation function

$R_{u_1 u_2 u_3}(\tau_1, \tau_2)$ which is abbreviated as $R_{121}(\tau_1, \tau_2)$ can be derived as

$$\begin{aligned}
 R_{121}(\tau_1, \tau_2) &= \sum_{i_1=1}^M \sum_{i_2=1}^M \sum_{i_3=1}^M \int_{-\infty}^{\infty} d\omega_1 \int_{-\infty}^{\infty} d\omega_2 \int_{-\infty}^{\infty} d\omega_3 \sum_{\substack{b: i_1 i_2 i_3 \\ s: i_1 i_2 i_3}} (s, \omega_1, \omega_2) \\
 &\quad \frac{G(\omega_1) G(\omega_2) G(-\omega_1 - \omega_2)}{-j^3 \lambda_1 \lambda_2 (\lambda_1^{-1} + \lambda_2^{-1})^{-1}} \exp[j(\tau_1 \omega_1 + \tau_2 \omega_2)] \\
 &\quad \left\langle \exp \left\{ j[b(\omega_1) + b(\omega_2) + b(-\omega_1 - \omega_2)] \right\} \right\rangle \\
 &\quad \int_{\pi_1} \frac{A_{i_1}(p_1)}{d_1'} \exp(-jk_1 d_1') dp_1 \int_{\pi_1} \frac{A_{i_2}(p_2)}{d_2} \exp(-jk_2 d_2) dp_2 \\
 &\quad \int_{\pi_1} \frac{A_{i_3}(p_3)}{d_3} \exp(j(k_1 + k_2)d_3) dp_3 \quad (3.4)
 \end{aligned}$$

where $d_1' = d(p_1, r_2)$ and $d_i = d(p_i, r_i)$ ($i = 2, 3$)

Then the cross-bispectral density $B_{121}(\omega_1, \omega_2)$, which is defined as the Fourier transform of $R_{121}(\tau_1, \tau_2)$, can be expressed as

$$\begin{aligned}
 & (1/2\pi)^2 \sum_{i_1=1}^M \sum_{i_2=1}^M \sum_{i_3=1}^M b_{S:i_1 i_2 i_3}(\omega_1, \omega_2) \frac{G(\omega_1)G(\omega_2)G(-\omega_1-\omega_2)}{-j^3 \lambda_1 \lambda_2 (\lambda_1^{-1} + \lambda_2^{-1})^{-1}} \\
 & \left\langle \exp \left\{ j[b(\omega_1) + b(\omega_2) + b(-\omega_1 - \omega_2)] \right\} \right\rangle \int_{\pi_1} \frac{A_{i_1}(p_1)}{d_1} \exp(-jk_1 d_1) dp_1 \\
 & \int_{\pi_1} \frac{A_{i_2}(p_2)}{d_2} \exp(-jk_2 d_2) dp_2 \int_{\pi_1} \frac{A_{i_3}(p_3)}{d_3} \exp(j(k_1 + k_2)d_3) dp_3
 \end{aligned} \tag{3.5}$$

In the same way, the auto-bispectral density $B_{111}(\omega_1, \omega_2)$ is obtained from Eq.(3.5) and is given below:

$$\begin{aligned}
 & B_{111}(\omega_1, \omega_2) \\
 & = (1/2\pi)^2 \sum_{i_1=1}^M \sum_{i_2=1}^M \sum_{i_3=1}^M b_{S:i_1 i_2 i_3}(\omega_1, \omega_2) \frac{G(\omega_1)G(\omega_2)G(-\omega_1-\omega_2)}{-j^3 \lambda_1 \lambda_2 (\lambda_1^{-1} + \lambda_2^{-1})^{-1}} \\
 & \left\langle \exp \left\{ j[b(\omega_1) + b(\omega_2) + b(-\omega_1 - \omega_2)] \right\} \right\rangle \int_{\pi_1} \frac{A_{i_1}(p_1)}{d_1} \exp(-jk_1 d_1) dp_1 \\
 & \int_{\pi_1} \frac{A_{i_2}(p_2)}{d_2} \exp(-jk_2 d_2) dp_2 \int_{\pi_1} \frac{A_{i_3}(p_3)}{d_3} \exp(j(k_1 + k_2)d_3) dp_3
 \end{aligned} \tag{3.6}$$

Equations (3.5) and (3.6) give the bispectra of the signals at the hologram plane and they are expressed as the product of the following three main terms: (i) the term which depends on the bispectrum of the object illuminating signals $s_i(p, t)$ ($i = 1, \dots, M$), (ii) the term due to the phase turbulence at three angular frequency components $\omega_1, \omega_2, \omega_3$

where $\omega_1 + \omega_2 + \omega_3 = 0$; and (iii) the object dependent term. In the expressions (3.5) and (3.6) the difference is only the use of d'_1 or d_1 ; thus if the ratio between them is taken, the other factors get cancelled.

Derivation of Hologram Signal from Bispectral Analysis: The data required for hologram signals are the relative amplitude and phase of the object waves at the hologram plane. They may be expressed as follows:

$$\begin{aligned} A_o(\omega; r) \exp[j\varphi_o(\omega; r)] &= \frac{A_s(\omega; r) \exp[j\varphi_s(\omega; r)]}{A_r(\omega; r) \exp[j\varphi_r(\omega; r)]} \\ &= \frac{A_s(\omega; r)}{A_r(\omega; r)} \exp[j(\varphi_s(\omega; r) - \varphi_r(\omega; r))] \end{aligned} \quad (3.7)$$

where $A_r \exp(j\varphi_r)$ is a reference wave and $A_s \exp(j\varphi_s)$ is the object wave at an observing or scanning point r on the plane.

Eqs. (3.5) and (3.6) show that the hologram signal at a scanning point r_2 can be immediately given by the following ratio:

$$\begin{aligned} \frac{B_{u:121}(\omega_1, \omega_2)}{B_{u:111}(\omega_1, \omega_2)} &= \frac{\sum_{i_1=1}^M \int_{\pi_1} \frac{A_{i1}(p_1)}{d'_1} \exp(-jk_1 d'_1) dp_1}{\sum_{i_1=1}^M \int_{\pi_1} \frac{A_{i1}(p_1)}{d_1} \exp(-jk_1 d_1) dp_1} \\ &= \hat{A}_o(\omega_1; r_2) \exp[i\hat{\varphi}_o(\omega_1; r_2)] \end{aligned} \quad (3.8)$$

where $B_{u:111}(\omega_1, \omega_2)$ is assumed to be non-zero.

Equation (3.8) implies that the hologram signal can be obtained as the ratio of the cross-bispectrum and auto-bispectrum of signals at two points on the hologram plane. In this expression, only the desired factors are obtained and the terms which depend on the bispectrum of the signal and the turbulences are cancelled because the ratio is used. Equation (3.8) also indicates that the result is free from additive Gaussian noises.

Image is reconstructed by carrying out the following operation:

$$|I(p')| = \left| \int_{\pi_2} \frac{\hat{A}_0(\omega_1; r)}{j\lambda_2 d(r, p')} \exp[j\hat{\phi}_0(\omega_1; r)] \exp[jk_2 d(r, p')] dr \right|$$

where p' denotes an image point to be reconstructed and $d(r, p')$ denotes the distance between r and p' .

3.2 The Computational Procedure Involved in Estimating the Bispectral Density

The signals detected by the scanning receiver and fixed receivers are $x_1(t)$ (object signal) and $x_2(t)$ (reference signal) respectively. Their third order correlation functions of $x_1(t)$ and $x_2(t)$ are assumed to be ergodic.

Then the third order auto-correlation function $x_q(t)$ ($q = 1, 2$) is defined as

$$R_{111}(\tau_1, \tau_2) = \lim_{T \rightarrow \infty} \frac{1}{T} \int_0^T x_1(t)x_1(t+\tau_1)x_1(t+\tau_2) dt$$

$$q = 1, 2$$

Hence observing the signal $x_q(t)$ ($q = 1, 2$) over a period T ,

one can compute

$$R_{111T}(\tau_1, \tau_2) = \frac{1}{T} \int_0^T x_q(t) x_q(t + \tau_1) x_q(t + \tau_2) dt$$

$$q = 1, 2$$

To compute $R_{111}(\tau_1, \tau_2)$, one has to observe the signal over many such intervals of time period T , and has to compute $R_{111T}(\tau_1, \tau_2)$ each time. Then the average of such $R_{111T}(\tau_1, \tau_2)$'s gives an estimate of $R_{111}(\tau_1, \tau_2)$, whose Fourier transform is nothing but an estimate of the auto-bispectral density of $x(t)$. An alternate way of doing this is to compute $B_{111T}(\omega_1, \omega_2)$ (Fourier transform of $R_{111T}(\tau_1, \tau_2)$) each time after observing the signal over a period T and then taking averages of such $B_{111T}(\omega_1, \omega_2)$'s. First we will see what is $B_{111T}(\omega_1, \omega_2)$ in terms of $X(\omega)$.

$B_{111T}(\omega_1, \omega_2)$ is defined as $F(R_{111T}(\tau_1, \tau_2))$ where $F(\cdot)$ denotes the Fourier transform. Therefore,

$$B_{111T}(\omega_1, \omega_2) = \frac{1}{T} \int_0^T \int_{-\infty}^{\infty} \int_{-\infty}^{\infty} x(t) x(t + \tau_1) x(t + \tau_2) e^{-j\omega_1 \tau_1} e^{-j\omega_2 \tau_2} dt d\tau_1 d\tau_2$$

$$= \frac{1}{T} \int_0^T \int_{-\infty}^{\infty} \int_{-\infty}^{\infty} x(t) x(\tau_1) e^{j\omega_1 t} x(\tau_2) e^{-j\omega_2 t} e^{-j\omega_1 \tau_1} e^{-j\omega_2 \tau_2} dt d\tau_1 d\tau_2$$

$$= \frac{1}{T} \int_{-\infty}^{\infty} x(\tau_1) e^{-j\omega_1 \tau_1} d\tau_1 \int_{-\infty}^{\infty} x(\tau_2) e^{-j\omega_2 \tau_2} d\tau_2 \int_0^T x(t) e^{j(\omega_1 + \omega_2)t} dt$$

[since $x(t)$ is observed only for an interval T , outside this interval its value is zero. Hence we can take the limits from $-\infty$ to $+\infty$]

$$= \frac{1}{T} x(\omega_1) x(\omega_2) x^*(\omega_1 + \omega_2)$$

The cross-bispectral density of $x_1(t)$ and $x_2(t)$ is defined as

$$B_{121}(\omega_1, \omega_2) = F(R_{121}(\tau_1, \tau_2))$$

To get an estimate of $B_{121}(\omega_1, \omega_2)$, the same procedure that is discussed above for estimating $B_{111}(\omega_1, \omega_2)$ is adapted here. Before actually going to the discussion of the computational procedure involved we will express $B_{121T}(\omega_1, \omega_2)$ in terms of $x_1(\omega)$ and $x_2(\omega)$.

$B_{121T}(\omega_1, \omega_2)$ is defined as $F(R_{121T}(\tau_1, \tau_2))$.

$$\begin{aligned} B_{121T}(\omega_1, \omega_2) &= \frac{1}{T} \int_0^T \int_{-\infty}^{\infty} \int_{-\infty}^{\infty} x_1(t) x_2(t+\tau_1) x_1(t+\tau_2) e^{-j\omega_1 \tau_1} e^{-j\omega_2 \tau_2} dt d\tau_1 d\tau_2 \\ &= \frac{1}{T} \int_0^T x_1(t) \int_{-\infty}^{\infty} x_2(t+\tau_1) e^{-j\omega_1 \tau_1} d\tau_1 \int_{-\infty}^{\infty} x_1(t+\tau_2) e^{-j\omega_2 \tau_2} d\tau_2 \\ &= \frac{1}{T} \int_0^T x_1(t) \int_{-\infty}^{\infty} x_2(\tau_1) e^{j\omega_1 t} e^{-j\omega_1 \tau_1} d\tau_1 \\ &\quad \int_{-\infty}^{\infty} x_1(\tau_2) e^{j\omega_2 t} e^{-j\omega_2 \tau_2} d\tau_2 \\ &= \frac{1}{T} \int_{-\infty}^{\infty} x_1(t) e^{j(\omega_1 + \omega_2)t} \int_{-\infty}^{\infty} x_2(\tau_1) e^{-j\omega_1 \tau_1} d\tau_1 \\ &\quad \int_{-\infty}^{\infty} x_1(\tau_2) e^{-j\omega_2 \tau_2} d\tau_2 \\ &= \frac{1}{T} x_2(\omega_1) x_1(\omega_2) x_1^*(\omega_1 + \omega_2) \end{aligned} \quad (3.23)$$

Thus the expressions for $B_{111T}(\omega_1, \omega_2)$, $B_{121T}(\omega_1, \omega_2)$ are derived, which are the triple products of the Fourier coefficients of $x_q(t)$ ($q = 1, 2$). Hence to get good estimates of $B_{111}(\omega_1, \omega_2)$ and $B_{121}(\omega_1, \omega_2)$ one has to average over many such triple products.

The computations may be surprisingly expensive despite the FFT. Moreover, all the pitfalls known from ordinary power spectrum analysis occur here too, some of them with new twists. Thus it seems worthwhile to describe and evaluate the different procedures in detail.

Assume that the bispectrum is to be estimated for frequencies between 0 and $\omega_0/2$ with a bandwidth Δ_0 . Hence a sampling rate of ω_0 samples per unit time is atleast needed and uninterrupted records whose size is atleast $N_0 = \omega_0/\Delta_0$. Prefiltering of the frequencies above $\omega_0/2$ is necessary to avoid aliasing. A total of K records (not necessarily consecutive), each of length $N = MN_0$ is assumed to be available. The value of N should be convenient for the FFT, say a power of 2 and M preferably is an odd integer ($M = 2L+1$). To satisfy both conditions a compromising value of N_0 may have to be chosen. Also, it may be necessary to adjust the records, either by adding zeroes at the ends or by allowing some overlap between consecutive records, to reach the exact length N; the final results will have to be corrected for these adjustments. The total number of points is of the order $N_{tot} = KN$.

Because of its symmetry, it suffices to estimate the bispectral density $B(\omega_1, \omega_2)$ in the triangle determined by the equalities.

$$0 \leq \omega_2 \leq \omega_1, \omega_1 + \omega_2 \leq \omega_0/2.$$

Number the records $j = 1, 2, \dots, k$. For each of them the following operations are performed:

- 1) Subtract the average and remove a linear trend if necessary.
- 2) Adding zeroes if necessary to obtain a convenient length N for the FFT.

Numbering the observations in the thus modified sample from 0 to $N-1$: $x_0 x_1 \dots x_{N-1}$

- 3) Fast Fourier transform is performed which gives the Fourier coefficients

$$X(\omega_k) = \sum_{i=0}^{N-1} x_i \exp(-j2\pi i k/N) \quad 0 \leq k \leq N/2$$

- 4) Estimate the bispectral density $B(\omega_1, \omega_2)$ at $(\omega_k, \omega_L) = \left(\frac{k\omega}{N}, \frac{L\omega}{N}\right)$ where $k, L = 0, 1, \dots, N/2$.

- a) Over a quadratic window

$$\hat{B}(\omega_1, \omega_2) \Delta_0^2 = \sum_{k_1=-L}^L \sum_{k_2=-L}^L X(\omega_1+k_1) X(\omega_2+k_2) X^*(\omega_1+\omega_2+k_1+k_2)$$

or more symmetrically,

- b) over a hexagonal window

$$\hat{B}(\omega_1, \omega_2) \Delta_0^2 = \frac{4M^2}{3M^2+1} \sum_{k_1=-L}^L \sum_{k_2=-L}^L X(\omega_1+k_1) X(\omega_2+k_2) X^*(\omega_1+\omega_2+k_1+k_2)$$

where the sum is extended over all k_1, k_2 satisfying

$$|k_1| \leq L, |k_2| \leq L, |k_1+k_2| \leq L$$

5) Finally, average over k pieces

$$\hat{B}(\omega_1, \omega_2) = \frac{1}{k} \sum_{j=1}^k B_j(\omega_1, \omega_2)$$

Part 4 is most expensive term in terms of computer time.

Procedure A: (Average in the Frequency domain): Evaluate operation 5 in the straightforward fashion, e.g. in case (a)

$$\hat{B}_j(\omega_1, \omega_2) \Delta_0^2 = \sum_{k_1=-L}^L X(\omega_1 + k_1) \sum_{k_2=-L}^L X^*(\omega_2 + k_2)$$

Procedure B: (Complex demodulation)

$$(1) \text{ Put } X^{\omega_L}(\omega_k) = X(\omega_L + \omega_k) \quad \text{for } |k| \leq L$$

$$= 0 \quad \text{otherwise}$$

$$X^{\omega_L}(\omega_k) = X(\omega_k + \omega_L) \quad \text{for } |k| \leq 2L$$

$$= 0 \quad \text{otherwise.}$$

This means that we apply a narrow band pass filter and shift frequencies to zero.

(2) Transform back-into the time domain. Let $n \geq 2M$ be the least number admitting an efficient FFT. Interpret index k modulo n and compute the finite Fourier transforms.

$$x^{\omega_L}(s) = \sum_K X^{\omega_L}(\omega_k) \exp(2\pi i sk/N)$$

and similarly for $X^{\omega_L}(\omega_k)$, giving $x^{\omega_L}(s)$.

3) Average in the time domain: In case (a) compute

$$\hat{B}_j(\omega_k, \omega_L) \Delta_o^2 = \frac{1}{n} \sum_{s=0}^{n-1} x^{\omega_k}(s) x^{\omega_L}(s) \tilde{x}^{(\omega_k + \omega_L)}(s)$$

In case (b) compute

$$\hat{B}_j(\omega_k, \omega_L) \Delta_o^2 = \frac{4M^2}{3M^2+1} \frac{1}{n} \sum_{s=0}^{n-1} x^{\omega_k}(s) \tilde{x}^{\omega_L}(s) x^{\omega_k + \omega_L}(s)$$

It is easy to see that this gives exactly same results as the straight forward evaluation of operation 4(a) or (b) respectively and this is more economical since one does not have to compute \tilde{X} and \tilde{x} .

The third window which is to be discussed is a good window. A good window is one which satisfies the following requirements:

- i) The variance of the estimate is as small as possible.
- ii) The width of the window must be as small as possible to reduce the computing costs
- iii) The window must be concentrated near the origin to reduce the bias of the estimate.

The window to be discussed is optimum in the sense that the bias of the estimate obtained by using this window is the minimum possible [5]. The variance of the estimate and computing costs are approximately the same in all the three cases. This optimum window in the time domain can be expressed as follows:

$$\omega_o(\tau_1, \tau_2) = d_o(\tau_1) d_o(\tau_2) d_o(\tau_2 - \tau_1)$$

where $d_o(\tau) = \frac{1}{\pi} |\sin(\pi\tau/M)| + (1 - \frac{|\tau|}{M}) \cos(\pi\tau/M)$

and the corresponding expression in frequency domain is as follows:

$$W_o(\omega_1, \omega_2) = \frac{1}{2\pi} \int_{-\infty}^{\infty} D_o(\omega_1 - y) D_o(\omega_2 + y) D_o(y) dy$$

$$\text{where } D_o(\omega) = 4M\pi^2 \frac{1 + \cos M}{(M^2 \omega^2 - \pi^2)^2}$$

where M is the maximum time lag of the window.

This window is used for estimating the bispectral density in this work.

Thus we have discussed the principle behind bispectral holography and estimation of bispectral density in this chapter.

CHAPTER 4

COMPUTER SIMULATION OF THE IMAGING MODEL

In the previous chapter the methodology for recording the hologram using bispectral analysis, and the computational aspects involved in the estimation of the bispectra were discussed. In this chapter the simulations that have been carried out for imaging the objects using bispectral analysis are given.

4.1 Image Reconstruction of a Point Source

The model used for computer simulation is shown in Fig. 4.1. Here the object considered is a point source. The signal emitted by the object is

$$S(t) = a_1 \cos(\omega t + \varphi) + a_2 \cos(2\omega t + \varphi) + a_3 \cos(4\omega t + \delta(t)) \quad (4.1)$$

where $\delta(t)$ is randomly fluctuated in time with uniform distribution over the range $(-\pi \text{ to } \pi)$. The signal chosen above is quasi-periodic, zero-mean and non-Gaussian. The noise that is added to the signal at the receivers is assumed to be Gaussian. The computer generated pseudo white Gaussian signal is taken as noise. The results of simulation for the power spectrum and bispectrum of the signal and noise are as follows. The power spectrum and bispectrum of both the signal and noise are computed. They are shown in Fig. 4.2, Fig.4.3 and Fig.4.4. The Figs. 4.3 and 4.4 are

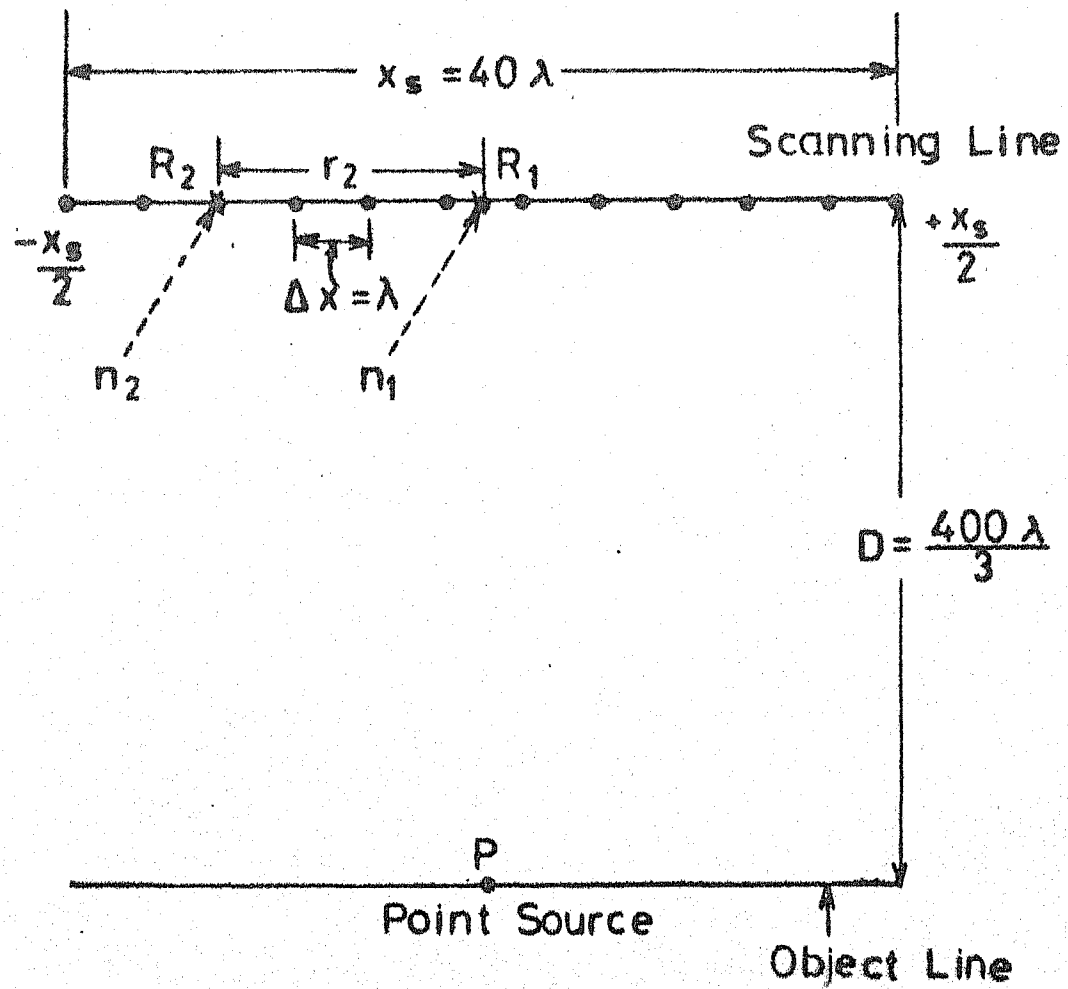


FIG.4.1 SET UP USED FOR THE RECONSTRUCTION OF THE IMAGE OF A POINT SOURCE

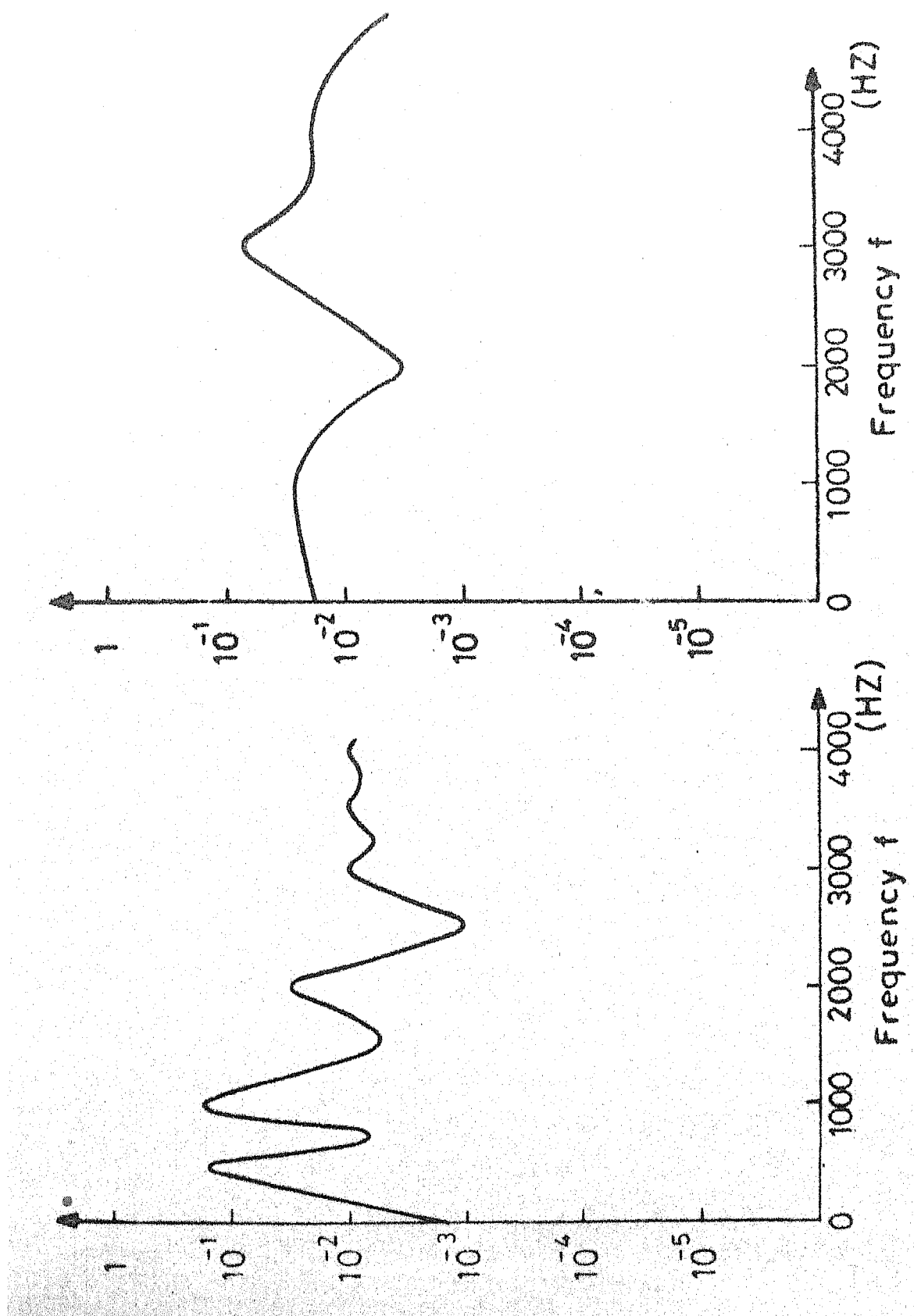


FIG. 4.2a POWER SPECTRAL DENSITY OF THE QUASI-PERIODIC NON-GAUSSIAN SIGNAL

FIG. 4.2b POWER SPECTRAL DENSITY OF THE COMPUTER GENERATED GAUSSIAN NOISE

48

Height of Blue Contours = 1×10^{-1}
Height of Black Contours = 1×10^{-2}
Bispectral density at the
point (500 Hz, 500 Hz) = 0.1853

5000 Hz

30

25

20

15

10

5

0

12

frequency

(500 Hz, 500 Hz)

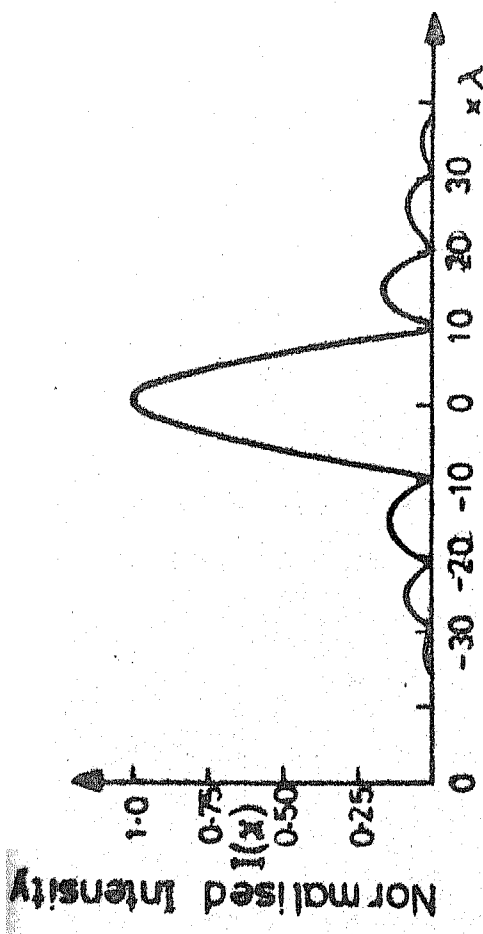
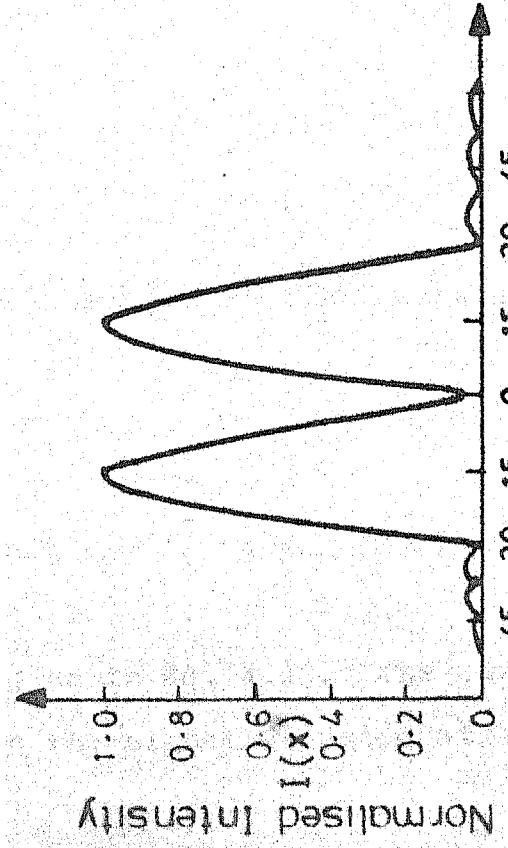
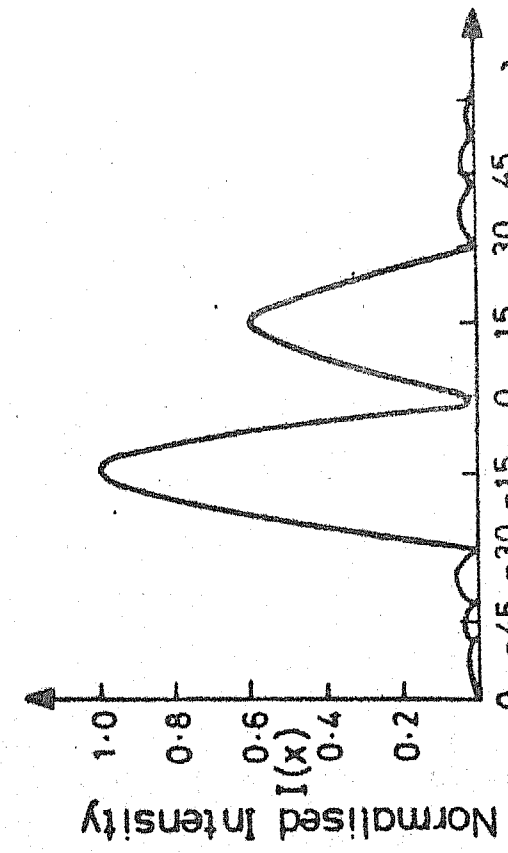


FIG. 4.5 (a) RECONSTRUCTED IMAGE OF A POINT SOURCE



(i)



(ii)

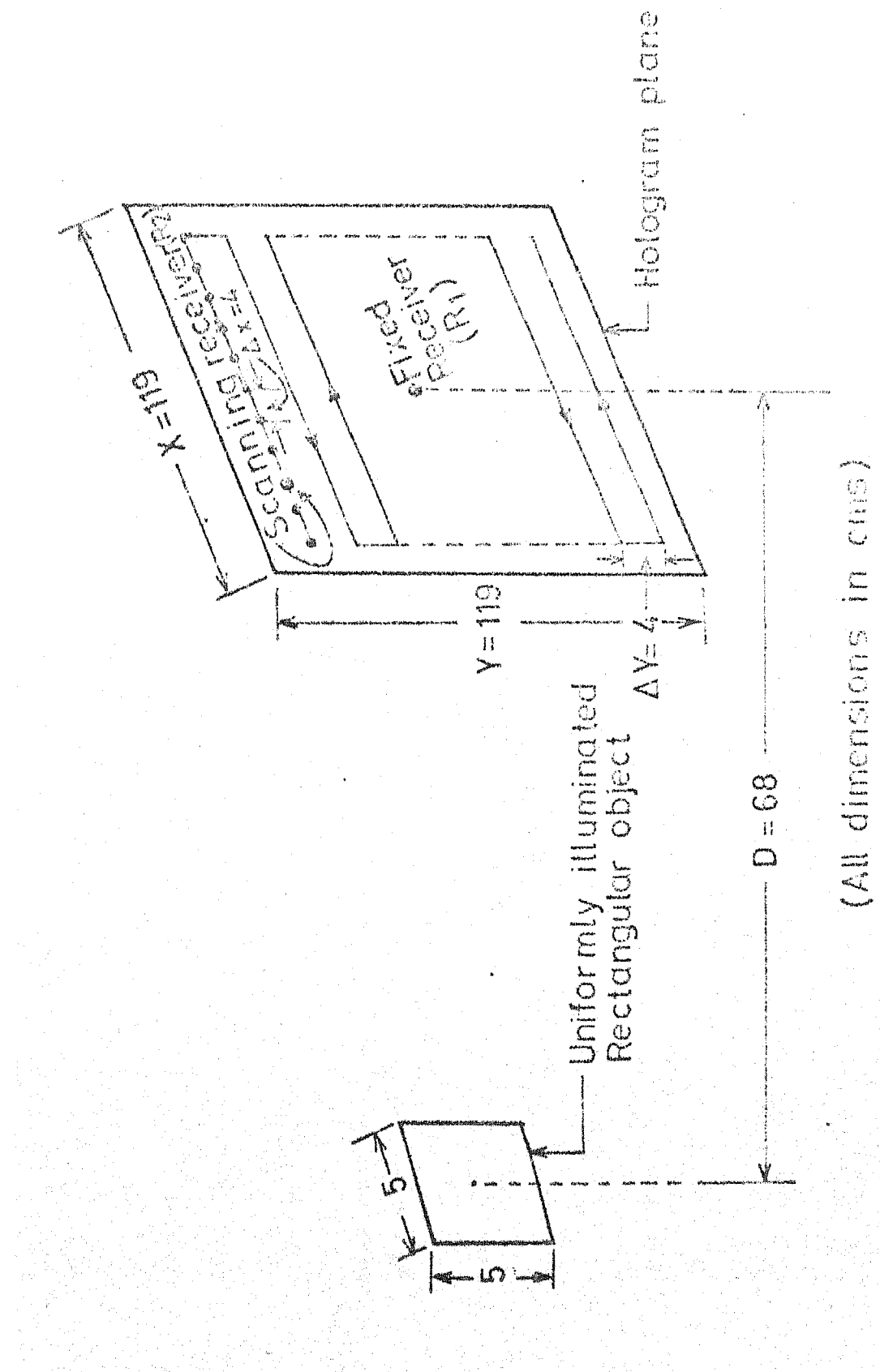
FIG. 4.5 (b) RECONSTRUCTED IMAGES OF TWO POINT SOURCES

4.2 Image Reconstruction of Two Adjacent Point Sources

The model used for simulation is similar to the one shown in Fig. 4.1, except for the fact that, two point sources are considered in the object plane instead of one. These two point sources are separated by a distance more than the resolution limit $2\lambda D/x_s$ where D is the distance of separation between the object line and scanning line. The same procedure as adapted in the case of a single point source is followed here. The reconstructed image is shown in Fig. 4.5 (b). In this figure reconstructed images for two cases are shown. In one case the two point sources are assumed to emit identical signals. In the other case it is assumed that the signals emitted by the two point sources are assumed to have different amplitude distributions. It is observed that the spacing between the two point sources in the reconstructed image is same as the spacing between the two point objects.

4.3 Image Reconstruction of an 'Uniformly Illuminated Patch'

The hologram considered here is a two dimensional one. Here also two detectors are employed, one fixed at the origin and the other scanning the hologram plane. The set up for this is shown in Fig. 4.6. The signal $x(t)$ emitted by the object is expressed as in Eq.(4.1). The contribution of the object signal to the signal detected at a point r



(All dimensions in cms.)

FIG. 4.6 "UNI-DIMENSIONAL Holography" using "GOMBE" Holography Unit (A) (B)

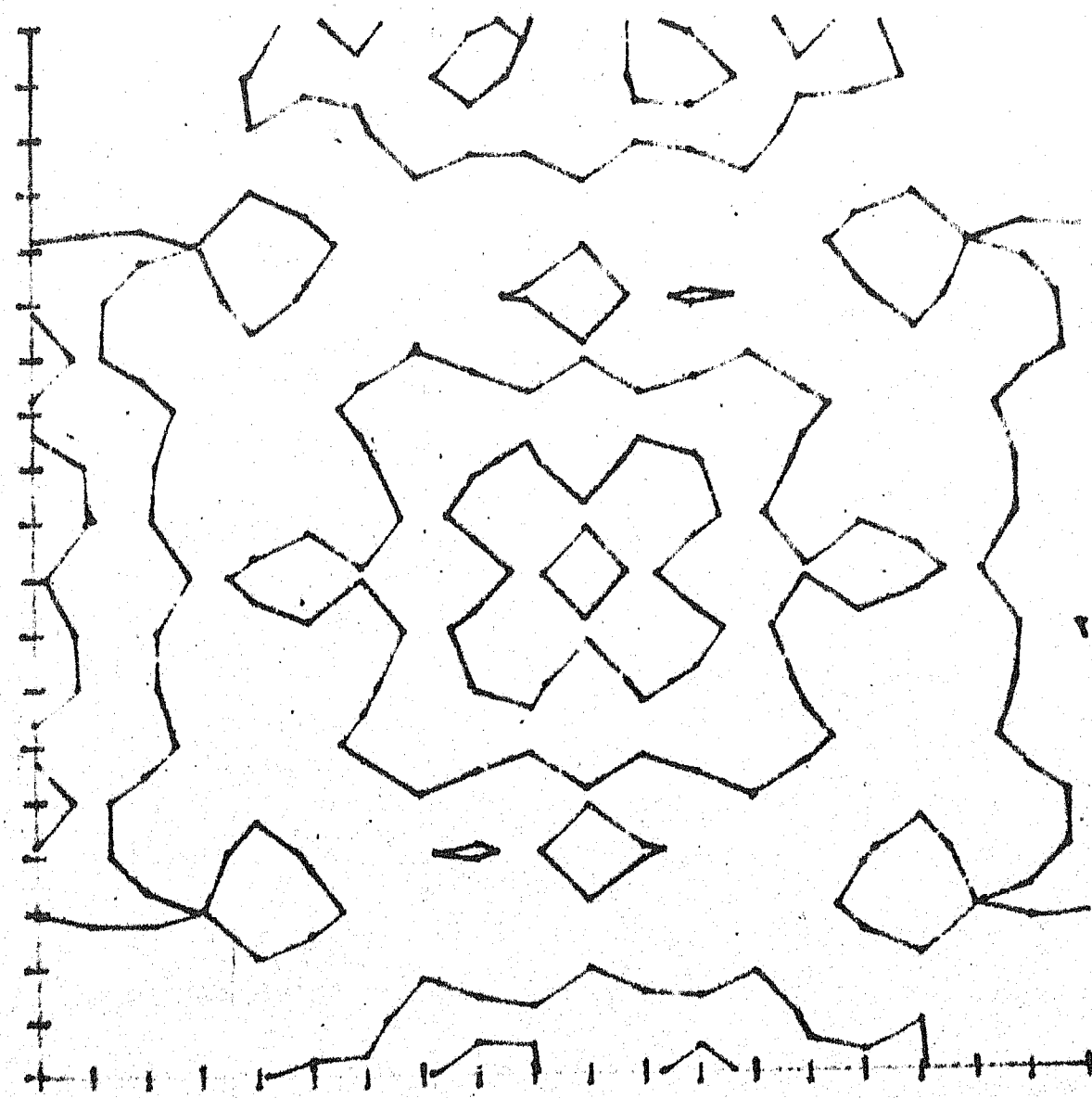


Fig 4.1 RECONSTRUCTED IMAGE OF THE OBJECT

"UNIFORMLY ILLUMINATED OBJECT"

on the hologram plane is obtained by integrating $x(t)$ over the whole object. As it takes more time to compute the integral, to find out the signal contribution the object is considered as a matrix (5 x 5) of point sources. Because of this fact the reconstructed image has slight intensity variations. The reconstructed image is shown in Fig. 4.7. It is obtained by contour mapping. All the contours shown in the figure correspond to same height. Since the variations in the intensities are very small, the contour of chosen intensity appear as shown in the figure. It is not giving a clear indication of the object. Because of that the reconstructed values of the image are also given in Tab. 4.1 which clearly gives the intensity variations.

In all the above cases, the medium considered causes only linear phase shift and attenuation.

The signal processing steps involved in the data acquisition and computer simulation of bispectral imaging technique are illustrated in Fig. 4.9.

Table 21.1

RECONSTRUCTED VALUES OF THE IMAGE

| | | | | | | | | | | | | | | | |
|------|------|------|------|------|------|------|------|------|------|------|------|------|------|------|------|
| 3.41 | 2.90 | 2.62 | 3.11 | 3.65 | 3.88 | 2.55 | 3.48 | 2.76 | 4.14 | 2.96 | 4.40 | 2.75 | 3.49 | 4.45 | 4.12 |
| 4.14 | 2.53 | 3.35 | 3.55 | 2.54 | 4.43 | 4.16 | 4.22 | 2.50 | 2.50 | 3.74 | 4.17 | 2.85 | 3.07 | 3.08 | 4.28 |
| 4.41 | 3.00 | 2.52 | 3.00 | 2.52 | 4.19 | 3.87 | 4.32 | 3.88 | 4.38 | 4.37 | 4.13 | 2.94 | 2.66 | 2.61 | 3.02 |
| 3.90 | 2.73 | 2.64 | 4.11 | 3.79 | 3.46 | 3.78 | 2.62 | 3.42 | 4.29 | 3.32 | 4.33 | 3.98 | 3.92 | 3.20 | 2.55 |
| 3.98 | 3.35 | 2.69 | 4.22 | 3.27 | 4.10 | 3.39 | 4.29 | 4.37 | 4.19 | 2.63 | 4.10 | 3.44 | 3.57 | 2.80 | 3.73 |
| 4.29 | 3.79 | 4.15 | 3.42 | 4.07 | 4.23 | 3.65 | 3.33 | 3.04 | 3.36 | 3.18 | 4.50 | 3.07 | 3.17 | 2.63 | 4.19 |
| 3.75 | 3.49 | 4.44 | 3.80 | 2.63 | 2.70 | 2.72 | 4.29 | 3.40 | 2.75 | 3.50 | 4.07 | 3.46 | 2.56 | 2.75 | 3.57 |
| 3.66 | 3.47 | 3.74 | 3.40 | 2.82 | 3.35 | 4.14 | 4.01 | 3.51 | 3.55 | 3.10 | 3.22 | 4.31 | 2.59 | 3.53 | 3.41 |
| 4.36 | 3.30 | 4.01 | 4.02 | 4.32 | 4.08 | 4.34 | 4.22 | 2.79 | 3.53 | 2.78 | 3.95 | 2.55 | 2.92 | 3.39 | 2.69 |
| 4.00 | 2.96 | 3.79 | 2.86 | 4.41 | 2.53 | 4.28 | 2.71 | 3.00 | 2.73 | 3.24 | 3.13 | 4.05 | 2.60 | 3.80 | 3.25 |
| 3.65 | 3.93 | 2.81 | 2.91 | 3.90 | 3.11 | 3.98 | 3.41 | 4.21 | 4.24 | 2.84 | 3.12 | 3.21 | 3.86 | 2.70 | 2.70 |
| 4.15 | 3.17 | 3.09 | 2.88 | 4.03 | 2.89 | 2.67 | 3.33 | 3.35 | 2.60 | 2.55 | 4.26 | 3.88 | 2.99 | 4.43 | 3.65 |
| 3.60 | 2.75 | 4.24 | 3.46 | 2.68 | 3.09 | 2.75 | 3.70 | 4.06 | 3.20 | 3.21 | 3.29 | 3.76 | 2.64 | 2.82 | 3.53 |
| 2.87 | 4.01 | 3.57 | 2.62 | 4.12 | 4.45 | 3.45 | 2.61 | 2.56 | 2.59 | 2.95 | 3.27 | 2.53 | 1.30 | 4.22 | 4.46 |
| 3.31 | 2.77 | 3.43 | 3.33 | 4.33 | 3.97 | 4.24 | 4.29 | 3.72 | 4.13 | 2.80 | 3.14 | 4.10 | 3.27 | 2.81 | 3.65 |
| 3.32 | 4.06 | 3.23 | 3.58 | 3.87 | 3.92 | 3.81 | 2.54 | 2.59 | 2.60 | 4.09 | 3.47 | 3.07 | 4.43 | 3.39 | 2.57 |
| 3.50 | 3.73 | 4.07 | 3.72 | 4.00 | 2.52 | 3.79 | 2.75 | 3.83 | 4.49 | 4.47 | 3.44 | 3.29 | 3.61 | 4.48 | 3.74 |
| 3.45 | 4.17 | 4.37 | 3.78 | 4.23 | 3.68 | 4.13 | 2.58 | 3.17 | 3.49 | 4.04 | 2.55 | 3.27 | 3.12 | 3.49 | 4.42 |
| 3.94 | 3.05 | 2.79 | 2.66 | 4.43 | 3.53 | 3.03 | 4.33 | 2.76 | 4.50 | 4.05 | 3.71 | 4.20 | 3.03 | 2.90 | 3.58 |
| 2.84 | 2.54 | 2.57 | 4.00 | 2.52 | 4.12 | 4.33 | 2.51 | 3.70 | 3.12 | 2.63 | 3.15 | 3.48 | 2.56 | 4.27 | 3.11 |

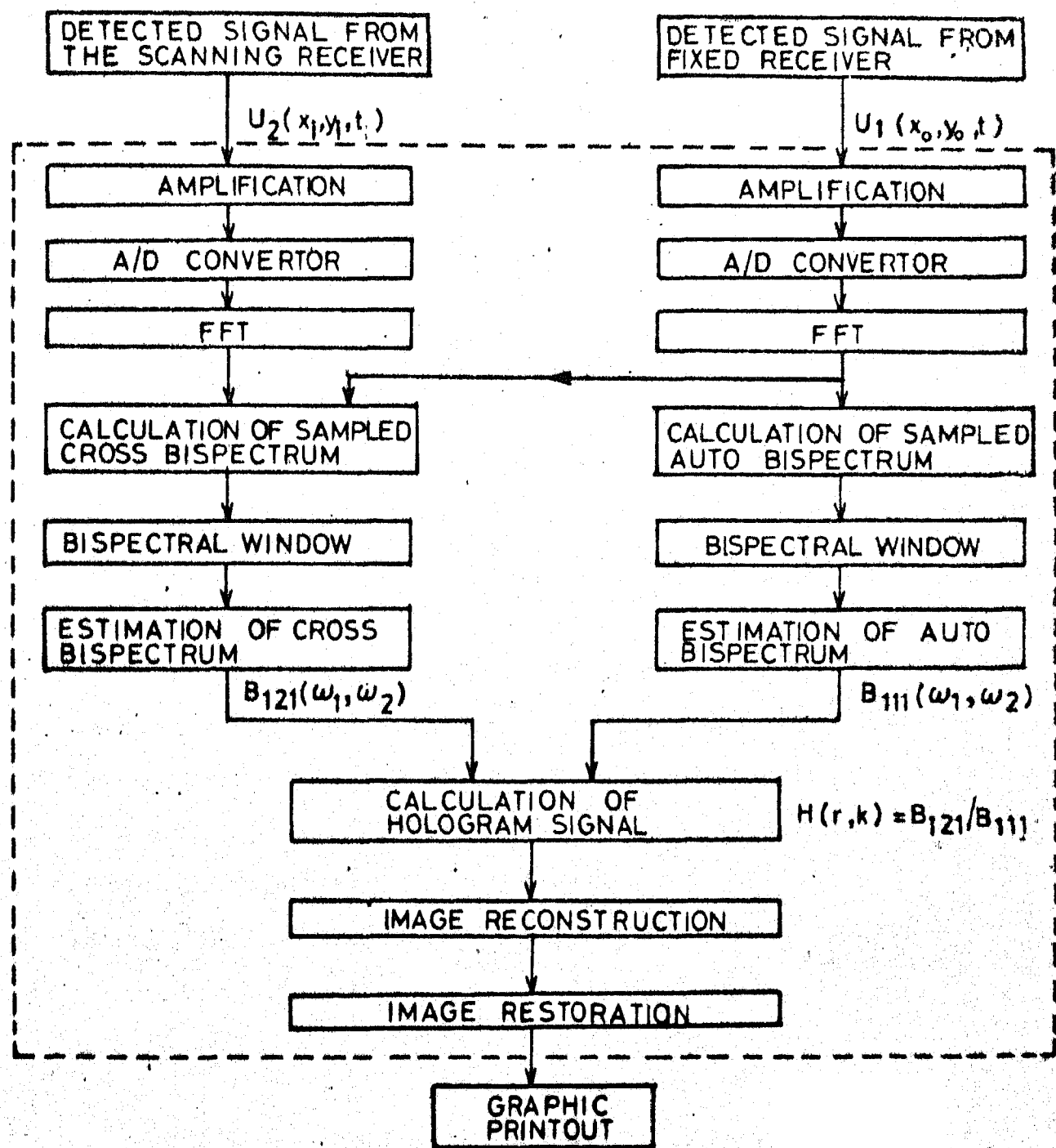


FIG. 4.9 SIGNAL PROCESSING STEPS IN BISPECTRAL HOLOGRAPHY

CHAPTER 5

CONCLUSIONS AND SUGGESTIONS

A study of the paper titled 'Bispectral Holography' by Takuso Sato and Kimio Sasaki initiated this work. After a brief discussion of the principles of holography and differences between the optical and acoustical holography, the technique of 'bispectral holography' as proposed by Sato and Sasaki is examined. A survey of the work carried out in this area is done. The fact that 'the bispectral analysis can eliminate the effects of noise and channel on the signal completely' is re-established using computer simulation with the help of three examples. In this work the channel is assumed to be 'deterministic'. Because of the immediate nonavailability of the information on realistic models of randomly turbulent media, no example pertaining to this case could be included, though the theory applies to this media also. This technique naturally requires more computation time than the conventional technique as one has to compute both the cross- and auto-bispectral densities of the scanned and reference signals and their ratio whereas in the conventional method one has to compute only the cross-power spectral density between the scanned and reference signals, for getting the hologram signal, but the advantages gained clearly justify the increased computation.

5.1 Suggestions for Future Work

Apart from its current applications to acoustic imaging, passive sonar [6] and machine system diagnosis [7], it is felt that the technique can be applied to problems of channel characterization and communications. This is elaborated in the following discussion.

a) Channel Characterization:

The procedure for channel characterization using the present method is as follows. A zero mean, non-Gaussian signal is transmitted through the channel to be characterized. Assume the corrupting noise to be additive Gaussian and statistically independent of the signal. The bispectrum of the received signal will be the bispectrum of the channel corrupted transmitted signal as the bispectrum of the noise becomes zero. The mathematical procedure for finding out the transfer function of the channel from the bispectrums of the transmitted and received signals is given below.

Let $h(t, \tau)$ be the impulse response of the linear time varying channel to be characterized. A known signal $x(t)$ is transmitted through the channel. It is assumed to be a quasi-periodic, non-Gaussian zero mean process. Its third order correlation function is assumed to be ergodic. The bispectral density of $x(t)$ is obtained by observing the signal $x(t)$ over a period T (T is sufficiently large to satisfy the ergodicity property and is given by

$$B_x(\omega_k, \omega_L) = \frac{1}{T} X(\omega_k) X(\omega_L) X^*(\omega_k + \omega_L) \quad (5.1)$$

The signal received at the other end of the channel is given by

$$\begin{aligned} Y(t) &= \int_{-\infty}^{\infty} x(\tau) h(t, \tau) d\tau + n(t) \\ &= m(t) + n(t) \end{aligned}$$

Assuming that $Y(t)$ is zero mean and its third order correlation function is ergodic, $R_y(\tau_1, \tau_2)$ is expressed as

$$\begin{aligned} &\frac{1}{T} \int_0^T y(t) y(t+\tau_1) y(t+\tau_2) \quad (\text{assuming } T \text{ is sufficiently large} \\ &\quad \text{to satisfy the ergodicity property}) \\ &= \frac{1}{T} \int_0^T m(t) m(t+\tau_1) m(t+\tau_2) \quad (\text{This is true under the assumption} \\ &\quad \text{that } m(t) \text{ and } n(t) \text{ are statistically independent}). \end{aligned}$$

$$\begin{aligned} \therefore B_y(\omega_k, \omega_L) &= \frac{1}{T} M(\omega_k) M(\omega_L) M^*(\omega_k + \omega_L) \\ &= \frac{1}{T} X(\omega_k) H(\omega_k, \tau) X(\omega_L) H(\omega_L, \tau) X^*(\omega_k + \omega_L) \\ &\quad H^*(\omega_k + \omega_L, \tau) \quad (5.2) \end{aligned}$$

(Assuming that the channel is not varying over the interval of observation) where τ is any time instant in the interval T . The ratio of Eqs.(5.1) and (5.2) gives

$$B_H(\omega_k, \omega_L, \tau) = H(\omega_k, \tau) H(\omega_L, \tau) H^*(\omega_k + \omega_L, \tau)$$

Evaluate $B_H(\omega_k, \omega_L, \tau)$ for $k, L = 1, 2, \dots, n$.

Then arranging these values in matrix form

$$\begin{bmatrix}
 H(\omega_1, \tau)H(\omega_1, \tau)H^*(\omega_1 + \omega_1, \tau) \dots & H(\omega_1, \tau)H(\omega_n, \tau)H^*(\omega_n + \omega_1, \tau) \\
 H(\omega_2, \tau)H(\omega_2, \tau)H^*(\omega_2 + \omega_2, \tau) & \\
 & \\
 H(\omega_n, \tau)H(\omega_1, \tau)H^*(\omega_n + \omega_1, \tau) & H(\omega_n, \tau)H(\omega_n, \tau)H^*(\omega_n + \omega_n, \tau)
 \end{bmatrix}$$

$$= \begin{bmatrix}
 B_H(\omega_1, \omega_1, \tau) & B_H(\omega_1, \omega_2, \tau) & B_H(\omega_1, \omega_n, \tau) \\
 & & \\
 B_H(\omega_2, \omega_2, \tau) & & \\
 & & \\
 & & \\
 B_H(\omega_n, \omega_n, \tau) & & B_H(\omega_n, \omega_n, \tau)
 \end{bmatrix}$$

To solve for $H(\omega_1, \tau), H(\omega_2, \tau) \dots, H(\omega_{2n}, \tau)$ there are only $\frac{n(n+1)}{2}$ equations since the above matrix is a symmetric matrix.

Since the above system is an over determined system of non-linear equations with multiplicative terms to find a solution one will have to first linearize them by taking the logarithm and then resorting to any one of the methods of solution for over determined system, e.g. pseudo inverse [16], least squares or residual projection method [17].

b) Communication through a Randomly Time Varying Media:

The image of the object reconstructed using bispectral analysis has the effect of neither the channel nor the additive

Gaussian noise. The bispectral analysis may be applied in the communications context where the aim is to obtain the signal free from additive noise and the effects of the channel. To get the image of the object the variation of the amplitude and phase of the object wave relative to those of the reference wave in space has to be determined whereas to get the signal transmitted, the variation of the amplitude and phase of the object signal with time has to be determined. For obtaining the signal, an analysis similar to the one used for getting image of the object can possibly be carried out by interchanging time and space domains.

APPENDIX

This contains some of the important listings of the computer simulation. Comment cards introduced in each routine explains the function of that routine.

REFERENCE S

1. B.P. Hildebrand and B.B. Brebden, 'An Introduction to Acoustical Holography', Plenum, New York, 1972.
2. Takuso Sato, Kimio Sasaki, 'Bispectral Holography', Journal of Acoustical Society of America, Vol.62, No.2, August 1977, pp. 404-408.
3. P.J. Huber, B.Kleiner, T. Gasser and G. Dummermuth, 'Statistical Methods for Investigating Phase Relations in Stationary Stochastic Process', IEEE Transactions on Audio and Electroacoustics, Au-19, 1971, pp. 78-86.
4. D.R. Brillinger, 'An Introduction to Polyspectra', Ann. Math. Stat. 36, 1965, pp. 36-46.
5. K. Sasaki, T. Sato and Y. Yamashita, 'Minimum Bias Windows for Bispectral Estimation', Journal of Sound and Vibrations- 40, 1975, pp. 139-148.
6. Kimio Sasaki, Takuso Sato and Yoichi Nakumura, 'Holographic Passive Sonar', IEEE Transactions on Sonics and Ultrasonics, Vol. SU-24, No.3, May 1977, pp. 193-200.
7. Takuso Sato, Kimio Sasaki and Masaharu Nonaka, 'Prototype of Bispectral Passive Imaging Systems Aiming Machine-System Diagnosis', Journal of Acoustical Society of America, 63(5), May 1978, pp. 1611-1616.
8. J.W. Vanness, 'Asymptotic Normality of Bispectral Estimates', Annals of Mathematical Statistics 37, 1966, pp. 1257-1272.

9. J.W. Goodman, 'Introduction to Fourier Optics', McGraw-Hill, New York, 1968, Chapter 8.
10. W.T. Cathey, 'Optical Information Processing and Holography', John Wiley and Sons, New York.
11. R.K. Otnes, L. Enochson, 'Applied Time Series Analysis', Vol.1, Wiley - Interscience Publication, New York.
12. V.I. Tatarski, 'Wave Propagation in a Turbulent Medium', Dover Publications, Inc. New York.
13. A. Gersho, 'Characterization of Time Varying Linear Systems', Research report, School of Electrical Engineering, Cornell University, Feb. 1963.
14. Kimio Sasaki and Takuso Sato, 'A Bispectral Synthesizer', Journal of Acoustical Society of America 65(3), March 1979.
15. Kimio Sasaki, Takuso Sato and Yoichi Nakumuru, 'An Effective Utilization of Spectral Spread in Holographic Passive Imaging Systems', IEEE Transactions on Sonics and Ultrasonics, Vol.Su-25, No.4, July 1978.
16. C.R. Rao and S.K. Mitra, 'Generalized Inverse of Matrices and its Applications', John Wiley and Sons, Inc., New York, 1971.

17. K. Tanabe, 'Projection Method for Solving a Singular System of Linear Equations and its Applications', *Numerische Mathematik*, 17, pp. 203-214, 1971.
18. Akira Ishimaru, 'Theory and Applications of Wave Propagation and Scattering in Random Media', *Proceedings of the IEEE*, July 1977, pp. 1030-1059.
19. E.V. Hoversten, R.O. Harger and S.J. Halme, 'Communication Theory for the Turbulent Atmosphere', *Proceedings of IEEE*, Special Issue on Optical Communication, Oct. 1970. pp. 1626-1649.
20. Anthony J. Devaney, 'Optical Coherence: Self-perpetuating Science', *Optical Spectra*, Oct. 1979, pp. 37-41.

卷之三

```

      T2=T1**2
      DSOP1=RX*SORT(D2+T2)
      DO 30 M=1,N
      RTM=FLOAT(M-1)/FLOAT(N)
      RM=2*PI*RTM
      Y(M)=COS(RM-DSOP1)+COS(2*RM+2*DSOP1+PHI)
      1+COS(4*RM-4*DSOP1+PHI)
      X(M)=CDSURM*DSOP2+COS(2*RM+PHI-2*DSOP2)
      1+COS(4*RM+PHI-4*DSOP2)
      CALL DDD(X,GAMM,N,INK,Z)
      CALL DDD(Y,GAMM,N,INK,Z)
      ABSD(K1)=Z(2)*Z(2)*CONJG(Z(3))
      CSD(K1)=Z(1)*Z(2)*CONJG(Z(3))
      HOST=CSD(K1)/ABSD(K1)
      HS(K1)=HOST
      CONTINUE
      JEO
      DD 98 1E-20,19
      JE0+
      88  RTM(ACT)=CONJG(HS(J))
      CALL FFTP( RTMA,40,INK1,INK,LS)
      PRINT400
      400  FORMAT(5X,'RECONSTRUCTED VALUES OF THE SIGNAL',/)
      DD 99 1E1,40
      99  XTM(ACT)=CABS( RTMA(1))
      PRINT700,(XTM(ACT),I=1,40)
      700  FORMAT(5X,SP15.8,/)
      119  CONTINUE
      STOP
      CALL FFTP
      CALL FFDRL2
      CALL FFT2
      END
      SUBROUTINE DDD(X,GAMM,N,INK,Z)
      IMPLICIT X(32),INK(61),YIMA(40)
      COMPLEX Z(32),GAMM,CNPLX
      N1=1/2
      N1=-1
      CALL FFTR(X,GAMM,N,INK)
      DO 50 I=1,N1,2
      50  X(I)=X(I)/
      GAMM=GMN/1
      K50
      DO 90 I=1,N1,2
      90  Z(I)=CNPLX(Y(I)),X(I+1))
      DO 70 I=2,N1
      70  Z(I+2)=CONJG(Z(I))
      Z(1+1)=GAMM
      DO 60 I=1,N1
      60  X(I)=(GAMM*Z(I+1))**2
      PR1=210
      2230 PRINT(5X,'POWER SPECTRAL DENSITY OF THE GIVEN SIGNAL',/)
      PR1111,X(I),I=1,N1
      2110 FORMAT(5X,SP15.8,/)
      RETURN
      END

```

```

100      A PROGRAMME FOR GENERATING THE BISPECTRAL DENSITY OF THE
105      GTFPA SIGNAL.
110      DIMENSION X(32),DX(64),TK(6),Y(32),V(4),TO(4)
115      COMPLEX Z(0:32),B(32,32),GAMN,CMPLX,Z2
120      COMMON/ARAL1/R
125      DATA V/1.,32./,1.,32./
130      DATA TO/0.5,1.1,0.3,0.9/
135      PT=32
140      PT=3,1415926535
145      R1=PI
150      R2=PI
155      SD=2.0
160      PH=0.52359
165      ISEED=21478364
170      T20.001/FLOAT(16)
175      P11.0/CMAT)
180      418N/FLOAT(2)
185      100  FORMAT(SX,'SAMPLED VALUES OF THE SIGNAL IN THE TIME DOMAIN',//)
190      105  FORMAT(SX,'SAMPLED VALUES OF THE NOISE IN THE TIME DOMAIN',//)
195      110  FORMAT(SX,'POWER SPECTRAL DENSITY OF THE GIVEN QUASI
200      115  PERIODIC NONGAUSSIAN SIGNAL',//)
205      120  FORMAT(SX,'POWER SPECTRAL DENSITY OF THE
210      125  GAUSSIAN NOISE',//)
215      130  FORMAT(SX,'SAMPLED VALUES OF THE BISPECTRAL DENSITY OF THE
220      135  THE GIVEN QUASI PERIODIC NONGAUSSIAN SIGNAL',//)
225      140  FORMAT(SX,'SAMPLED VALUES OF THE BISPECTRAL DENSITY OF THE
230      145  THE COMPUTER GENERATED NOISE',//)
235      150  FORMAT(SX,'B00 000 13)
240      155  FORMAT(12.4(2F15.6))
245      160  103  FORMAT(SX,'SIGNAL TO NOISE RATIO= ',//)
250      165  108  100  GENERATING THE SAMPLED VALUES OF THE NOISE IN THE TIME
255      170  110  DOMAIN.
260      175  115  CALL CGNP(ISEED,V,V)
265      180  120  DO 123 I=1,6
270      185  125  123  V=(1.0-1.00*V(1))
275      190  130  125  V=PI*10.0*(V(1),1=1,6)
280      195  135  125  CALL PATE(Y,V,GAMN,1,TK)
285      200  140  135  V=PI*10.0*(V(1),1=1,6)
290      205  145  135  CALL B00(V,V)
295      210  150  135  CALL D00(V,V)
300      215  155  135  STOP
305      220  160  135

```



```

NDIVX=32
NDIVY=32
IFORM(1)=1
IFORM(2)=5
JHSZ=1/10
NOCHENDCH/8
NOCVENDCV/8
OTHRX=1
OTHRY=1
N=32
DO 99 I=1,2
ACCEPT*,CBEG,CLIM,CSTP
CALL LINE(1,1,0)
CALL AXES(-1,1,32.,-1,1,32.)
RV=0.
IX=0
DO 88 J=0,31,5
RV=FLOAT(J)-0.5
CALL LINE(RV,-3.,0)
IX=J
88 CALL CHAR(IX,21)
CALL LINE(2,75,5,5,0)
CALL CHAR("X560HZ",2)
IY=0
DO 77 K=0,31,5
RY=FLOAT(K)
CALL LINE(-5.,RY,0)
IY=K
77 CALL CHAR(IY,21)
CALL LINE(-1,32.,0)
CALL CHAR("X560HZ",2)
CALL LINE(-20.,15.,0)
CALL CHAR("FREQUENCY F24.",)
CALL LINE(7.5,-7.5,0)
CALL CHAR("FREQUENCY F14.",)
CALL LINE(1.5,-10.,0)
CALL CHAR("SPECTRAL DENSITY.",)
CALL LINE(16.,-10.,0)
CALL CHAR("OF THE NOISE.",)
CALL LINE(1.,1.,0)
CALL COMB(1,1,1,1,CBEG,CLIM,CSTP)
CALL LINE(1.,1.,0)
CONTINUE
RETURN
END

```

SUBROUTINE CONTR(NDIM1,NDIM2,NUSD1,NUSD2,CBEG,CUM,CSTR)
 PLOTS CONTOURS OF SPECIFIED HEIGHTS THRU GIVEN TWO-DIMENSIONAL
 ADHAY DATA.
 CONTOUR HEIGHTS PLOTTED ARE CTR=CBEG,CBEG+STEP,CBEG+2*STEP,
 SO LONG AS CTR DOES NOT EXCEED CUM EITHER WHILE INCREASING OR
 DECREASING. STEP IS CSTR WITH THE SIGN OF CUM-CBEG. ONLY
 CTR>CBEG IS PLOTTED IF CSTR>0.
 DATA WAS DIMENSIONED NDIM1 BY NDIM2 IN A DIMENSION STATEMENT IN
 THE CALLING PROGRAM, BUT ONLY THE FIRST NUSD1 BY NUSD2 ARE
 ACTUALLY USED. (FIRST SUBSCRIPT MUST INCREASE FASTEST IN STORAGE
 ORDER, AS USUAL). ALL ACTUAL PLOTTING IS DONE IN THE USER-
 SUPPLIED SUBROUTINE CPLOT, WHICH MUST BE HEADED AS FOLLOWS--
 SUBROUTINE CPLOT(X1,X2,CTR)
 CONTR EXTRUDES ONE POINT AT A TIME TO CPLOT. (X1,X2) IS THE
 COORDINATE PAIR, X1 FROM 1.0 TO FLOAT(NUSD1), X2 FROM
 1.0 TO FLOAT(NUSD2). IF DESIRED FOR EFFICIENCY, CPLOT MAY
 SAVE UP POINTS IN A WORK ARRAY.
 FOR IPLOT=0, CPLOT SHOULD JUST REMEMBER THIS POINT (MOVE TO
 (X1,X2) WITH PEN UP FOR A CALCOMP PLOTTER).
 FOR IPLOT=1, CPLOT SHOULD DRAW A LINE SEGMENT FROM THE LAST POINT
 TO THE CURRENT POINT AND REMEMBER THE CURRENT POINT (MOVE TO
 (X1,X2) WITH PEN DOWN).
 FOR IPLOT=2, CPLOT SHOULD PLOT A NUMERIC LABEL GIVING THE VALUE
 OF CTR AT THIS POINT. EACH PHYSICALLY SEPARATE CONTOUR DRAWN
 WILL RECEIVE ONE LABEL.
 EACH DATUM IS INCREASED BY 1.E-20 AND ALTERED IN ITS TWO LOW ORDER
 BITS. NON-ZERO FLOATING POINT VALUES ARE HARDLY AFFECTED, THOUGH
 FIXED POINT VALUES MIGHT BE. (CONVERT TO FIXED POINT BY SAYING--
 INTEGER DATA,CTR1,CTR2,CTR3
 AND CHANGING ABS(DATA)=INT(TABS(DATA)).
 DIMENSION NUSD(2),IX(2),IA(2),IB(2),IDEL(2),IFORB(2)
 1,K1(2),XFIRST(2),XPAREV(2),YFIRST(2),XSEC(2),XDIV(2)
 DIMENSION DATA(400)
 COMPLEX BC20/201
 COMMON/AREA1/R
 R=20

```

    NUSD1=20
    NUSD2=20
    CBEG=0
    DO 1 I=1,1
    DO 2 J=1,1
    2 Z=941
    DATA(99)=REAL(BC(1,1))*1000000
    CPLOT(X1,X2,CTR)
    NUSD1=NUSD1
    NUSD2=NUSD2
    CTR=CBEG
    DO 3 I=1,NDIM1
    3 DO 4 J=1,NDIM2
    4 IF(ABS(DATA(I,J))<1.E-20) THEN
    5 DO 6 I=1,NDIM1
    6 DO 7 J=1,NDIM2
    7 IF(ABS(DATA(I,J))<1.E-20) THEN
    8 DO 9 I=1,NDIM1
    9 DO 10 J=1,NDIM2
    10 IF(ABS(DATA(I,J))<1.E-20) THEN
    11 DO 12 I=1,NDIM1
    12 DO 13 J=1,NDIM2
    13 IF(ABS(DATA(I,J))<1.E-20) THEN
    14 DO 15 I=1,NDIM1
    15 DO 16 J=1,NDIM2
    16 IF(ABS(DATA(I,J))<1.E-20) THEN
    17 DO 18 I=1,NDIM1
    18 DO 19 J=1,NDIM2
    19 IF(ABS(DATA(I,J))<1.E-20) THEN
    20 DO 21 I=1,NDIM1
    21 DO 22 J=1,NDIM2
    22 IF(ABS(DATA(I,J))<1.E-20) THEN
    23 DO 24 I=1,NDIM1
    24 DO 25 J=1,NDIM2
    25 IF(ABS(DATA(I,J))<1.E-20) THEN
    26 DO 27 I=1,NDIM1
    27 DO 28 J=1,NDIM2
    28 IF(ABS(DATA(I,J))<1.E-20) THEN
    29 DO 30 I=1,NDIM1
    30 DO 31 J=1,NDIM2
    31 IF(ABS(DATA(I,J))<1.E-20) THEN
    32 DO 33 I=1,NDIM1
    33 DO 34 J=1,NDIM2
    34 IF(ABS(DATA(I,J))<1.E-20) THEN
    35 DO 36 I=1,NDIM1
    36 DO 37 J=1,NDIM2
    37 IF(ABS(DATA(I,J))<1.E-20) THEN
    38 DO 39 I=1,NDIM1
    39 DO 40 J=1,NDIM2
    40 IF(ABS(DATA(I,J))<1.E-20) THEN
    41 DO 42 I=1,NDIM1
    42 DO 43 J=1,NDIM2
    43 IF(ABS(DATA(I,J))<1.E-20) THEN
    44 DO 45 I=1,NDIM1
    45 DO 46 J=1,NDIM2
    46 IF(ABS(DATA(I,J))<1.E-20) THEN
    47 DO 48 I=1,NDIM1
    48 DO 49 J=1,NDIM2
    49 IF(ABS(DATA(I,J))<1.E-20) THEN
    50 DO 51 I=1,NDIM1
    51 DO 52 J=1,NDIM2
    52 IF(ABS(DATA(I,J))<1.E-20) THEN
    53 DO 54 I=1,NDIM1
    54 DO 55 J=1,NDIM2
    55 IF(ABS(DATA(I,J))<1.E-20) THEN
    56 DO 57 I=1,NDIM1
    57 DO 58 J=1,NDIM2
    58 IF(ABS(DATA(I,J))<1.E-20) THEN
    59 DO 60 I=1,NDIM1
    60 DO 61 J=1,NDIM2
    61 IF(ABS(DATA(I,J))<1.E-20) THEN
    62 DO 63 I=1,NDIM1
    63 DO 64 J=1,NDIM2
    64 IF(ABS(DATA(I,J))<1.E-20) THEN
    65 DO 66 I=1,NDIM1
    66 DO 67 J=1,NDIM2
    67 IF(ABS(DATA(I,J))<1.E-20) THEN
    68 DO 69 I=1,NDIM1
    69 DO 70 J=1,NDIM2
    70 IF(ABS(DATA(I,J))<1.E-20) THEN
    71 DO 72 I=1,NDIM1
    72 DO 73 J=1,NDIM2
    73 IF(ABS(DATA(I,J))<1.E-20) THEN
    74 DO 75 I=1,NDIM1
    75 DO 76 J=1,NDIM2
    76 IF(ABS(DATA(I,J))<1.E-20) THEN
    77 DO 78 I=1,NDIM1
    78 DO 79 J=1,NDIM2
    79 IF(ABS(DATA(I,J))<1.E-20) THEN
    80 DO 81 I=1,NDIM1
    81 DO 82 J=1,NDIM2
    82 IF(ABS(DATA(I,J))<1.E-20) THEN
    83 DO 84 I=1,NDIM1
    84 DO 85 J=1,NDIM2
    85 IF(ABS(DATA(I,J))<1.E-20) THEN
    86 DO 87 I=1,NDIM1
    87 DO 88 J=1,NDIM2
    88 IF(ABS(DATA(I,J))<1.E-20) THEN
    89 DO 90 I=1,NDIM1
    90 DO 91 J=1,NDIM2
    91 IF(ABS(DATA(I,J))<1.E-20) THEN
    92 DO 93 I=1,NDIM1
    93 DO 94 J=1,NDIM2
    94 IF(ABS(DATA(I,J))<1.E-20) THEN
    95 DO 96 I=1,NDIM1
    96 DO 97 J=1,NDIM2
    97 IF(ABS(DATA(I,J))<1.E-20) THEN
    98 DO 99 I=1,NDIM1
    99 DO 100 J=1,NDIM2
    100 IF(ABS(DATA(I,J))<1.E-20) THEN
    101 DO 102 I=1,NDIM1
    102 DO 103 J=1,NDIM2
    103 IF(ABS(DATA(I,J))<1.E-20) THEN
    104 DO 105 I=1,NDIM1
    105 DO 106 J=1,NDIM2
    106 IF(ABS(DATA(I,J))<1.E-20) THEN
    107 DO 108 I=1,NDIM1
    108 DO 109 J=1,NDIM2
    109 IF(ABS(DATA(I,J))<1.E-20) THEN
    110 DO 111 I=1,NDIM1
    111 DO 112 J=1,NDIM2
    112 IF(ABS(DATA(I,J))<1.E-20) THEN
    113 DO 114 I=1,NDIM1
    114 DO 115 J=1,NDIM2
    115 IF(ABS(DATA(I,J))<1.E-20) THEN
    116 DO 117 I=1,NDIM1
    117 DO 118 J=1,NDIM2
    118 IF(ABS(DATA(I,J))<1.E-20) THEN
    119 DO 120 I=1,NDIM1
    120 DO 121 J=1,NDIM2
    121 IF(ABS(DATA(I,J))<1.E-20) THEN
    122 DO 123 I=1,NDIM1
    123 DO 124 J=1,NDIM2
    124 IF(ABS(DATA(I,J))<1.E-20) THEN
    125 DO 126 I=1,NDIM1
    126 DO 127 J=1,NDIM2
    127 IF(ABS(DATA(I,J))<1.E-20) THEN
    128 DO 129 I=1,NDIM1
    129 DO 130 J=1,NDIM2
    130 IF(ABS(DATA(I,J))<1.E-20) THEN
    131 DO 132 I=1,NDIM1
    132 DO 133 J=1,NDIM2
    133 IF(ABS(DATA(I,J))<1.E-20) THEN
    134 DO 135 I=1,NDIM1
    135 DO 136 J=1,NDIM2
    136 IF(ABS(DATA(I,J))<1.E-20) THEN
    137 DO 138 I=1,NDIM1
    138 DO 139 J=1,NDIM2
    139 IF(ABS(DATA(I,J))<1.E-20) THEN
    140 DO 141 I=1,NDIM1
    141 DO 142 J=1,NDIM2
    142 IF(ABS(DATA(I,J))<1.E-20) THEN
    143 DO 144 I=1,NDIM1
    144 DO 145 J=1,NDIM2
    145 IF(ABS(DATA(I,J))<1.E-20) THEN
    146 DO 147 I=1,NDIM1
    147 DO 148 J=1,NDIM2
    148 IF(ABS(DATA(I,J))<1.E-20) THEN
    149 DO 150 I=1,NDIM1
    150 DO 151 J=1,NDIM2
    151 IF(ABS(DATA(I,J))<1.E-20) THEN
    152 DO 153 I=1,NDIM1
    153 DO 154 J=1,NDIM2
    154 IF(ABS(DATA(I,J))<1.E-20) THEN
    155 DO 156 I=1,NDIM1
    156 DO 157 J=1,NDIM2
    157 IF(ABS(DATA(I,J))<1.E-20) THEN
    158 DO 159 I=1,NDIM1
    159 DO 160 J=1,NDIM2
    160 IF(ABS(DATA(I,J))<1.E-20) THEN
    161 DO 162 I=1,NDIM1
    162 DO 163 J=1,NDIM2
    163 IF(ABS(DATA(I,J))<1.E-20) THEN
    164 DO 165 I=1,NDIM1
    165 DO 166 J=1,NDIM2
    166 IF(ABS(DATA(I,J))<1.E-20) THEN
    167 DO 168 I=1,NDIM1
    168 DO 169 J=1,NDIM2
    169 IF(ABS(DATA(I,J))<1.E-20) THEN
    170 DO 171 I=1,NDIM1
    171 DO 172 J=1,NDIM2
    172 IF(ABS(DATA(I,J))<1.E-20) THEN
    173 DO 174 I=1,NDIM1
    174 DO 175 J=1,NDIM2
    175 IF(ABS(DATA(I,J))<1.E-20) THEN
    176 DO 177 I=1,NDIM1
    177 DO 178 J=1,NDIM2
    178 IF(ABS(DATA(I,J))<1.E-20) THEN
    179 DO 180 I=1,NDIM1
    180 DO 181 J=1,NDIM2
    181 IF(ABS(DATA(I,J))<1.E-20) THEN
    182 DO 183 I=1,NDIM1
    183 DO 184 J=1,NDIM2
    184 IF(ABS(DATA(I,J))<1.E-20) THEN
    185 DO 186 I=1,NDIM1
    186 DO 187 J=1,NDIM2
    187 IF(ABS(DATA(I,J))<1.E-20) THEN
    188 DO 189 I=1,NDIM1
    189 DO 190 J=1,NDIM2
    190 IF(ABS(DATA(I,J))<1.E-20) THEN
    191 DO 192 I=1,NDIM1
    192 DO 193 J=1,NDIM2
    193 IF(ABS(DATA(I,J))<1.E-20) THEN
    194 DO 195 I=1,NDIM1
    195 DO 196 J=1,NDIM2
    196 IF(ABS(DATA(I,J))<1.E-20) THEN
    197 DO 198 I=1,NDIM1
    198 DO 199 J=1,NDIM2
    199 IF(ABS(DATA(I,J))<1.E-20) THEN
    200 DO 201 I=1,NDIM1
    201 DO 202 J=1,NDIM2
    202 IF(ABS(DATA(I,J))<1.E-20) THEN
    203 DO 204 I=1,NDIM1
    204 DO 205 J=1,NDIM2
    205 IF(ABS(DATA(I,J))<1.E-20) THEN
    206 DO 207 I=1,NDIM1
    207 DO 208 J=1,NDIM2
    208 IF(ABS(DATA(I,J))<1.E-20) THEN
    209 DO 210 I=1,NDIM1
    210 DO 211 J=1,NDIM2
    211 IF(ABS(DATA(I,J))<1.E-20) THEN
    212 DO 213 I=1,NDIM1
    213 DO 214 J=1,NDIM2
    214 IF(ABS(DATA(I,J))<1.E-20) THEN
    215 DO 216 I=1,NDIM1
    216 DO 217 J=1,NDIM2
    217 IF(ABS(DATA(I,J))<1.E-20) THEN
    218 DO 219 I=1,NDIM1
    219 DO 220 J=1,NDIM2
    220 IF(ABS(DATA(I,J))<1.E-20) THEN
    221 DO 222 I=1,NDIM1
    222 DO 223 J=1,NDIM2
    223 IF(ABS(DATA(I,J))<1.E-20) THEN
    224 DO 225 I=1,NDIM1
    225 DO 226 J=1,NDIM2
    226 IF(ABS(DATA(I,J))<1.E-20) THEN
    227 DO 228 I=1,NDIM1
    228 DO 229 J=1,NDIM2
    229 IF(ABS(DATA(I,J))<1.E-20) THEN
    230 DO 231 I=1,NDIM1
    231 DO 232 J=1,NDIM2
    232 IF(ABS(DATA(I,J))<1.E-20) THEN
    233 DO 234 I=1,NDIM1
    234 DO 235 J=1,NDIM2
    235 IF(ABS(DATA(I,J))<1.E-20) THEN
    236 DO 237 I=1,NDIM1
    237 DO 238 J=1,NDIM2
    238 IF(ABS(DATA(I,J))<1.E-20) THEN
    239 DO 240 I=1,NDIM1
    240 DO 241 J=1,NDIM2
    241 IF(ABS(DATA(I,J))<1.E-20) THEN
    242 DO 243 I=1,NDIM1
    243 DO 244 J=1,NDIM2
    244 IF(ABS(DATA(I,J))<1.E-20) THEN
    245 DO 246 I=1,NDIM1
    246 DO 247 J=1,NDIM2
    247 IF(ABS(DATA(I,J))<1.E-20) THEN
    248 DO 249 I=1,NDIM1
    249 DO 250 J=1,NDIM2
    250 IF(ABS(DATA(I,J))<1.E-20) THEN
    251 DO 252 I=1,NDIM1
    252 DO 253 J=1,NDIM2
    253 IF(ABS(DATA(I,J))<1.E-20) THEN
    254 DO 255 I=1,NDIM1
    255 DO 256 J=1,NDIM2
    256 IF(ABS(DATA(I,J))<1.E-20) THEN
    257 DO 258 I=1,NDIM1
    258 DO 259 J=1,NDIM2
    259 IF(ABS(DATA(I,J))<1.E-20) THEN
    260 DO 261 I=1,NDIM1
    261 DO 262 J=1,NDIM2
    262 IF(ABS(DATA(I,J))<1.E-20) THEN
    263 DO 264 I=1,NDIM1
    264 DO 265 J=1,NDIM2
    265 IF(ABS(DATA(I,J))<1.E-20) THEN
    266 DO 267 I=1,NDIM1
    267 DO 268 J=1,NDIM2
    268 IF(ABS(DATA(I,J))<1.E-20) THEN
    269 DO 270 I=1,NDIM1
    270 DO 271 J=1,NDIM2
    271 IF(ABS(DATA(I,J))<1.E-20) THEN
    272 DO 273 I=1,NDIM1
    273 DO 274 J=1,NDIM2
    274 IF(ABS(DATA(I,J))<1.E-20) THEN
    275 DO 276 I=1,NDIM1
    276 DO 277 J=1,NDIM2
    277 IF(ABS(DATA(I,J))<1.E-20) THEN
    278 DO 279 I=1,NDIM1
    279 DO 280 J=1,NDIM2
    280 IF(ABS(DATA(I,J))<1.E-20) THEN
    281 DO 282 I=1,NDIM1
    282 DO 283 J=1,NDIM2
    283 IF(ABS(DATA(I,J))<1.E-20) THEN
    284 DO 285 I=1,NDIM1
    285 DO 286 J=1,NDIM2
    286 IF(ABS(DATA(I,J))<1.E-20) THEN
    287 DO 288 I=1,NDIM1
    288 DO 289 J=1,NDIM2
    289 IF(ABS(DATA(I,J))<1.E-20) THEN
    290 DO 291 I=1,NDIM1
    291 DO 292 J=1,NDIM2
    292 IF(ABS(DATA(I,J))<1.E-20) THEN
    293 DO 294 I=1,NDIM1
    294 DO 295 J=1,NDIM2
    295 IF(ABS(DATA(I,J))<1.E-20) THEN
    296 DO 297 I=1,NDIM1
    297 DO 298 J=1,NDIM2
    298 IF(ABS(DATA(I,J))<1.E-20) THEN
    299 DO 300 I=1,NDIM1
    300 DO 301 J=1,NDIM2
    301 IF(ABS(DATA(I,J))<1.E-20) THEN
    302 DO 303 I=1,NDIM1
    303 DO 304 J=1,NDIM2
    304 IF(ABS(DATA(I,J))<1.E-20) THEN
    305 DO 306 I=1,NDIM1
    306 DO 307 J=1,NDIM2
    307 IF(ABS(DATA(I,J))<1.E-20) THEN
    308 DO 309 I=1,NDIM1
    309 DO 310 J=1,NDIM2
    310 IF(ABS(DATA(I,J))<1.E-20) THEN
    311 DO 312 I=1,NDIM1
    312 DO 313 J=1,NDIM2
    313 IF(ABS(DATA(I,J))<1.E-20) THEN
    314 DO 315 I=1,NDIM1
    315 DO 316 J=1,NDIM2
    316 IF(ABS(DATA(I,J))<1.E-20) THEN
    317 DO 318 I=1,NDIM1
    318 DO 319 J=1,NDIM2
    319 IF(ABS(DATA(I,J))<1.E-20) THEN
    320 DO 321 I=1,NDIM1
    321 DO 322 J=1,NDIM2
    322 IF(ABS(DATA(I,J))<1.E-20) THEN
    323 DO 324 I=1,NDIM1
    324 DO 325 J=1,NDIM2
    325 IF(ABS(DATA(I,J))<1.E-20) THEN
    326 DO 327 I=1,NDIM1
    327 DO 328 J=1,NDIM2
    328 IF(ABS(DATA(I,J))<1.E-20) THEN
    329 DO 330 I=1,NDIM1
    330 DO 331 J=1,NDIM2
    331 IF(ABS(DATA(I,J))<1.E-20) THEN
    332 DO 333 I=1,NDIM1
    333 DO 334 J=1,NDIM2
    334 IF(ABS(DATA(I,J))<1.E-20) THEN
    335 DO 336 I=1,NDIM1
    336 DO 337 J=1,NDIM2
    337 IF(ABS(DATA(I,J))<1.E-20) THEN
    338 DO 339 I=1,NDIM1
    339 DO 340 J=1,NDIM2
    340 IF(ABS(DATA(I,J))<1.E-20) THEN
    341 DO 342 I=1,NDIM1
    342 DO 343 J=1,NDIM2
    343 IF(ABS(DATA(I,J))<1.E-20) THEN
    344 DO 345 I=1,NDIM1
    345 DO 346 J=1,NDIM2
    346 IF(ABS(DATA(I,J))<1.E-20) THEN
    347 DO 348 I=1,NDIM1
    348 DO 349 J=1,NDIM2
    349 IF(ABS(DATA(I,J))<1.E-20) THEN
    350 DO 351 I=1,NDIM1
    351 DO 352 J=1,NDIM2
    352 IF(ABS(DATA(I,J))<1.E-20) THEN
    353 DO 354 I=1,NDIM1
    354 DO 355 J=1,NDIM2
    355 IF(ABS(DATA(I,J))<1.E-20) THEN
    356 DO 357 I=1,NDIM1
    357 DO 358 J=1,NDIM2
    358 IF(ABS(DATA(I,J))<1.E-20) THEN
    359 DO 360 I=1,NDIM1
    360 DO 361 J=1,NDIM2
    361 IF(ABS(DATA(I,J))<1.E-20) THEN
    362 DO 363 I=1,NDIM1
    363 DO 364 J=1,NDIM2
    364 IF(ABS(DATA(I,J))<1.E-20) THEN
    365 DO 366 I=1,NDIM1
    366 DO 367 J=1,NDIM2
    367 IF(ABS(DATA(I,J))<1.E-20) THEN
    368 DO 369 I=1,NDIM1
    369 DO 370 J=1,NDIM2
    370 IF(ABS(DATA(I,J))<1.E-20) THEN
    371 DO 372 I=1,NDIM1
    372 DO 373 J=1,NDIM2
    373 IF(ABS(DATA(I,J))<1.E-20) THEN
    374 DO 375 I=1,NDIM1
    375 DO 376 J=1,NDIM2
    376 IF(ABS(DATA(I,J))<1.E-20) THEN
    377 DO 378 I=1,NDIM1
    378 DO 379 J=1,NDIM2
    379 IF(ABS(DATA(I,J))<1.E-20) THEN
    380 DO 381 I=1,NDIM1
    381 DO 382 J=1,NDIM2
    382 IF(ABS(DATA(I,J))<1.E-20) THEN
    383 DO 384 I=1,NDIM1
    384 DO 385 J=1,NDIM2
    385 IF(ABS(DATA(I,J))<1.E-20) THEN
    386 DO 387 I=1,NDIM1
    387 DO 388 J=1,NDIM2
    388 IF(ABS(DATA(I,J))<1.E-20) THEN
    389 DO 390 I=1,NDIM1
    390 DO 391 J=1,NDIM2
    391 IF(ABS(DATA(I,J))<1.E-20) THEN
    392 DO 393 I=1,NDIM1
    393 DO 394 J=1,NDIM2
    394 IF(ABS(DATA(I,J))<1.E-20) THEN
    395 DO 396 I=1,NDIM1
    396 DO 397 J=1,NDIM2
    397 IF(ABS(DATA(I,J))<1.E-20) THEN
    398 DO 399 I=1,NDIM1
    399 DO 400 J=1,NDIM2
    400 IF(ABS(DATA(I,J))<1.E-20) THEN
    401 DO 402 I=1,NDIM1
    402 DO 403 J=1,NDIM2
    403 IF(ABS(DATA(I,J))<1.E-20) THEN
    404 DO 405 I=1,NDIM1
    405 DO 406 J=1,NDIM2
    406 IF(ABS(DATA(I,J))<1.E-20) THEN
    407 DO 408 I=1,NDIM1
    408 DO 409 J=1,NDIM2
    409 IF(ABS(DATA(I,J))<1.E-20) THEN
    410 DO 411 I=1,NDIM1
    411 DO 412 J=1,NDIM2
    412 IF(ABS(DATA(I,J))<1.E-20) THEN
    413 DO 414 I=1,NDIM1
    414 DO 415 J=1,NDIM2
    415 IF(ABS(DATA(I,J))<1.E-20) THEN
    416 DO 417 I=1,NDIM1
    417 DO 418 J=1,NDIM2
    418 IF(ABS(DATA(I,J))<1.E-20) THEN
    419 DO 420 I=1,NDIM1
    420 DO 421 J=1,NDIM2
    421 IF(ABS(DATA(I,J))<1.E-20) THEN
    422 DO 423 I=1,NDIM1
    423 DO 424 J=1,NDIM2
    424 IF(ABS(DATA(I,J))<1.E-20) THEN
    425 DO 426 I=1,NDIM1
    426 DO 427 J=1,NDIM2
    427 IF(ABS(DATA(I,J))<1.E-20) THEN
    428 DO 429 I=1,NDIM1
    429 DO 430 J=1,NDIM2
    430 IF(ABS(DATA(I,J))<1.E-20) THEN
    431 DO 432 I=1,NDIM1
    432 DO 433 J=1,NDIM2
    433 IF(ABS(DATA(I,J))<1.E-20) THEN
    434 DO 435 I=1,NDIM1
    435 DO 436 J=1,NDIM2
    436 IF(ABS(DATA(I,J))<1.E-20) THEN
    437 DO 438 I=1,NDIM1
    438 DO 439 J=1,NDIM2
    439 IF(ABS(DATA(I,J))<1.E-20) THEN
    440 DO 441 I=1,NDIM1
    441 DO 442 J=1,NDIM2
    442 IF(ABS(DATA(I,J))<1.E-20) THEN
    443 DO 444 I=1,NDIM1
    444 DO 445 J=1,NDIM2
    445 IF(ABS(DATA(I,J))<1.E-20) THEN
    446 DO 447 I=1,NDIM1
    447 DO 448 J=1,NDIM2
    448 IF(ABS(DATA(I,J))<1.E-20) THEN
    449 DO 450 I=1,NDIM1
    450 DO 451 J=1,NDIM2
    451 IF(ABS(DATA(I,J))<1.E-20) THEN
    452 DO 453 I=1,NDIM1
    453 DO 454 J=1,NDIM2
    454 IF(ABS(DATA(I,J))<1.E-20) THEN
    455 DO 456 I=1,NDIM1
    456 DO 457 J=1,NDIM2
    457 IF(ABS(DATA(I,J))<1.E-20) THEN
    458 DO 459 I=1,NDIM1
    459 DO 460 J=1,NDIM2
    460 IF(ABS(DATA(I,J))<1.E-20) THEN
    461 DO 462 I=1,NDIM1
    462 DO 463 J=1,NDIM2
    463 IF(ABS(DATA(I,J))<1.E-20) THEN
    464 DO 465 I=1,NDIM1
    465 DO 466 J=1,NDIM2
    466 IF(ABS(DATA(I,J))<1.E-20) THEN
    467 DO 468 I=1,NDIM1
    468 DO 469 J=1,NDIM2
    469 IF(ABS(DATA(I,J))<1.E-20) THEN
    470 DO 471 I=1,NDIM1
    471 DO 472 J=1,NDIM2
    472 IF(ABS(DATA(I,J))<1.E-20) THEN
    473 DO 474 I=1,NDIM1
    474 DO 475 J=1,NDIM2
    475 IF(ABS(DATA(I,J))<1.E-20) THEN
    476 DO 477 I=1,NDIM1
    477 DO 478 J=1,NDIM2
    478 IF(ABS(DATA(I,J))<1.E-20) THEN
    479 DO 480 I=1,NDIM1
    480 DO 481 J=1,NDIM2
    481 IF(ABS(DATA(I,J))<1.E-20) THEN
    482 DO 483 I=1,NDIM1
    483 DO 484 J=1,NDIM2
    484 IF(ABS(DATA(I,J))<1.E-20) THEN
    485 DO 486 I=1,NDIM1
    486 DO 487 J=1,NDIM2
    487 IF(ABS(DATA(I,J))<1.E-20) THEN
    488 DO 489 I=1,NDIM1
    489 DO 490 J=1,NDIM2
    490 IF(ABS(DATA(I,J))<1.E-20) THEN
    491 DO 492 I=1,NDIM1
    492 DO 493 J=1,NDIM2
    493 IF(ABS(DATA(I,J))<1.E-20) THEN
    494 DO 495 I=1,NDIM1
    495 DO 496 J=1,NDIM2
    496 IF(ABS(DATA(I,J))<1.E-20) THEN
    497 DO 498 I=1,NDIM1
    498 DO 499 J=1,NDIM2
    499 IF(ABS(DATA(I,J))<1.E-20) THEN
    500 DO 501 I=1,NDIM1
    501 DO 502 J=1,NDIM2
    502 IF(ABS(DATA(I,J))<1.E-20) THEN
    503 DO 504 I=1,NDIM1
    504 DO 505 J=1,NDIM2
    505 IF(ABS(DATA(I,J))<1.E-20) THEN
    506 DO 507 I=1,NDIM1
    507 DO 508 J=1,NDIM2
    508 IF(ABS(DATA(I,J))<1.E-20) THEN
    509 DO 510 I=1,NDIM1
    510 DO 511 J=1,NDIM2
    511 IF(ABS(DATA(I,J))<1.E-20) THEN
    512 DO 513 I=1,NDIM1
    513 DO 514 J=1,NDIM2
    514 IF(ABS(DATA(I,J))<1.E-20) THEN
    515 DO 516 I=1,NDIM1
    516 DO 517 J=1,NDIM2
    517 IF(ABS(DATA(I,J))<1.E-20) THEN
    518 DO 519 I=1,NDIM1
    519 DO 520 J=1,NDIM2
    520 IF(ABS(DATA(I,J))<1.E-20) THEN
    521 DO 522 I=1,NDIM1
    522 DO 523 J=1,NDIM2
    523 IF(ABS(DATA(I,J))<1.E-20) THEN
    524 DO 525 I=1,NDIM1
    525 DO 526 J=1,NDIM2
    526 IF(ABS(DATA(I,J))<1.E-20) THEN
    527 DO 528 I=1,NDIM1
    528 DO 529 J=1,NDIM2
    529 IF(ABS(DATA(I,J))<1.E-20) THEN
    530 DO 531 I=1,NDIM1
    531 DO 532 J=1,NDIM2
    532 IF(ABS(DATA(I,J))<1.E-20) THEN
    533 DO 534 I=1,NDIM1
    534 DO 535 J=1,NDIM2
   
```



```

160 APREV(1)=X(1)
170 APREV(2)=X(2)
180 X(1)=EXTENT(1)
190 X(2)=EXTENT(2)
200 IF(TDIR>180)190,190
210 CALL CPLOT(IPHAS/4,XFRST(1),XFRST(2),CTR)
220 IPIRE=0
230 CALL CPLOT(IPHAS/2,X(1),X(2),CTR)
240 GO TO (200,210,350,380,390),IPHAS
250 IPHAS=2
260 DO 220 I=1,2
270 IX(I)=XC(I)+EPS
280 XDIF(I)=X(I)-FLOAT(TX(I))-EPS
290 IFORBD(I)=(IX(I)+NHSD(I)-4)/(NHSD(I)-2)-1
300 IF(TDIR>240,230,230
310 DX=IX(I)+NDTM1*(IX(2)-1)
320 BOTH DIRECTIONS ARE MARKED IF THE CONTOUR PASSES THRU THE CORNER
330 CALL MARKLOC(DATA(LX),IVARY,XDIF(IVARY))
340 ****
350 LOOK IN ALL EIGHT POSSIBLE DIRECTIONS FROM THE CURRENT CROSSING
360 FOR ANOTHER CROSSING. LOOK IN THE CURRENT DIRECTION FIRST, AT
370 ADJACENT SEGMENTS TO PREVENT FIGURE EIGHTS.
380 IVARY=3-IVARY
390 IUPRV=IVARY
400 DO 330 LOOK=1,8
410 ON 290 IVORY=1,2
420 IF(CDTP(IVORY)>250,250,270
430 IGNORE SEGMENTS OUTSIDE DATA OR WHICH INCLUDE THE CURRENT CROSSING
440 IF(IDELT(IVORY)=IFORB(IVORY))260,300,260
450 IF(IVORY)=1+IV(IVORY)+IDELT(IVORY)
460 GO TO 290
470 IF(IDELT(IVORY)+1=IVARY+IVORY)280,300,280
480 IF(IVORY)=1+IV(IVORY)+(TDIRP(IVORY)+1)/2
490 IF(IVORY)=1+IV(IVORY)
500 IF(IVARY)=1+IV(IVARY)-IDELT(IVARY)
510 IVARY=3-IVARY
520 GO TO 50
530 IDELT(1UPRV)=-IDELT(1UPRV)
540 ON 1,2,330,310,330,320,330,310,330,320,1,LOOK
550 IVARY=3-IVARY
560 GO TO 330
570 IUPRV=3-1UPRV
580 IDELT(1UNVP)=-IDELT(1UNVP)
590 ON 1,2,3
600 ****
610 AND THIS CONTOUR SEGMENT IF ALL DIRECTIONS FROM HERE HAVE BEEN
620 SPANNED. AT MOST ONE CONNECTING POINT OR A LABEL IS NOW PLOTTED.
630 IF(IPHAS>2)380,340,350
640 IVY CLOSING THE CONTOUR TO A NEARBY(LX)EXCEPT THE PREVIOUS)CROSSING
650 ICHAS=1
660 CHASCP
670 GO TO 240
680 PRINT A CONTOUR LABEL AT THE END OF THIS CONTOUR
690 IF(IPHAS>2)390,390,360
700 IF(CLOSE(1)=XFRST(1)+XFRST(2)*XFRST(2)-XFRST(1)*EPS)370,370,140
710 IF(CLOSE(X(1)-XFRST(1)+XFRST(2)*XFRST(2)-XFRST(1)*EPS)370,370,140

```

```

370 1 PHASE=5
2   LF(XPRev(2))180,180,180
3   IF THE CONTOUR HAS NOT CLOSED ON ITSELF, RETURN TO THE STARTING
4   POINT AND SEARCH FOR CONTINUATION IN ANOTHER DIRECTION
380 1PHASE=2
2   CTRD=CTRZ
3   IDIP=1
4   X(1)=XPRev(1)
5   X(2)=XPRev(2)
6   XPRRev(1)=XSEC(1)
7   XPRRev(2)=XSEC(2)
8   GO TO 210
9   390 CONTINUE
C   ****
10  IF(CSTP)400,410,400
11  CTR=CTR+SIGN(CSTP,CLIM-CBEG)
12  IF((CTR-CLIM)*SIGN(1.,CLIM-CBEG)=-.001*ABS(CSTP))110,10,410
13  IN CASE SUBROUTINE CPLOT IS SAYING UP POINTS, CLEAR IT OUT
14  CALL CPLOT(0,1,1,0.)
15  RETURN
16  END
17  SUBROUTINE ZERLOC(ADATA)
18  SET THE TWO LOW ORDER BITS OF ADATA TO ZERO
19  1PH 360 READ4 OR INTEGER*4.
20  (X=ITYA(ADATA))
21  CONTINUE
22  IF(IAD) 30,21,30
23  IX=4*(IX/4)
24  ADATA=ADATFLOAT(IX)
25  ATDATA=FLOAT(IX)
26  RETURN
27  END
28  SUBROUTINE TPLCITN(TDATA,IVARY)
29  RETURN 0 IF BIT IVARY (1 OR 2) OF TDATA IS 0,1 IF NOT.
30  17=TDATA
31  RDATA=5*(17*T/41)
32  IX=17*IX(RDATA)
33  IF(IXK,EO,33) GO TO 20
34  IF(IVARY,EO,IX) GO TO 20
35  IX=0
36  GO TO 30
37  18=1
38  RETURN
39  END
40  SUBROUTINE MKLOC(ADATA,IVARY,DTD)
41  SET BIT IVARY(1 OR 2) OF ADATA TO 1, (TO BE CALLED ONLY ONCE
42  PER POINT). SET BOTH LOW ORDER BITS TO 1 IF DTD =0.
43  19=160 READ4 OR INTEGER*4
44  UT=DATA(160,IVARY)
45  IF(UT)20,10,20
46  CTD=DATA(161,IVARY)
47  DT=DATA(162,IVARY)
48  RETURN
49  END
50  SUBROUTINE CPLOT(X1,X2,CTR)
51  IF(CPLOT=13) 13,33,45
52  CALL CPLOT(X1,X2,IPLOT)
53  GO TO 45

```

Abbey

Date Slip A 66956

This book is to be returned on the
date last stamped.

A blank ledger page with a vertical column header and a horizontal row header. The page is divided into two main sections by a vertical line in the center. The top section is labeled 'CD' and the bottom section is labeled '6.72.9'. The page contains several horizontal dotted lines for recording data.

CD 6.72.9

EE-1980-M-RED-ACO